Osteology of the archosauromorph Teyujagua paradoxa and the early evolution of the archosauriform skull

Pinheiro, Felipe; Oliveira, Daniel; Butler, Richard

DOI:
10.1093/zoolinnean/zlz093

The Linnean Society of London
ZOOLOGICAL Journal of the Linnean Society

Osteology of the archosauromorph *Teyujagua paradoxa* Pinheiro et al. 2016 and the early evolution of the archosauriform skull

Journal:	*Zoological Journal of the Linnean Society*
Manuscript ID	ZOJ-03-2019-3638.R1
Manuscript Type:	Original Article
Keywords:	Archosauromorpha < Taxa, Gondwana < Palaeontology, Triassic < Palaeontology, phylogeny < Phylogenetics, skull < Anatomy
Abstract:	Archosauriformes are a major group of reptiles that include the crown group Archosauria (birds, crocodilians, and their extinct relatives) and closely related taxa. Archosauriformes are characterized by a highly diagnostic skull architecture, which is linked to the predatory habits of their early representatives and the development of extensive cranial pneumaticity associated with the nasal capsule. The evolution of the archosauriform skull from the more plesiomorphic configuration present ancestrally in the broader clade Archosauromorpha was, until recently, elusive. This began to change with the discovery and description of *Teyujagua paradoxa*, an early archosauromorph from the Lower Triassic Sanga do Cabral Formation of Brazil. Here, we provide a detailed osteological description of the holotype and thus far only known specimen of *T. paradoxa*. In addition to providing new details of the anatomy of *T. paradoxa*, our study also revealed an early development of skull pneumaticity prior to the emergence of the antorbital fenestra. We use this new data to discuss the evolution of antorbital openings within Archosauriformes. Reappraisal of the phylogenetic position of *T. paradoxa* supports previous hypotheses of a close relationship with Archosauriformes. The data presented here provide new insights into character evolution during the origin of the archosauriform skull.

Archosauriformes are a major group of fossil and living reptiles that include the crown group Archosauria (birds, crocodilians, and their extinct relatives) and closely related taxa. Archosauriformes are characterized by a highly diagnostic skull architecture, which is linked to the predatory habits of their early representatives and the development of extensive cranial pneumaticity associated with the nasal capsule. The evolution of the archosauriform skull from the more plesiomorphic configuration present ancestrally in the broader clade Archosauromorpha was, until recently, elusive. This began to change with the discovery and description of *Teyujagua paradoxa*, an early archosauromorph from the Lower Triassic Sanga do Cabral Formation of Brazil. Here, we provide a detailed osteological description of the holotype and thus far only known specimen of *T. paradoxa*. In addition to providing new details of the anatomy of *T. paradoxa*, our study also reveals an early development of skull pneumaticity prior to the emergence of the antorbital fenestra. We use these new data to discuss the evolution of antorbital openings within Archosauriformes. Reappraisal of the phylogenetic position of *T. paradoxa* supports previous hypotheses of a close relationship with Archosauriformes. The data presented here provide new insights into character evolution during the origin of the archosauriform skull.

ADDITIONAL KEYWORDS: Archosauromorpha – Brazil – Gondwana – Lower Triassic – phylogeny – skull.

INTRODUCTION

Archosauriformes are an extraordinarily diverse clade of diapsid reptiles that originated during the Permian and underwent several pulses of adaptive radiation during the Mesozoic Era (Gauthier, 1986; Brusatte et al., 2008; Claessens et al., 2009; Nesbitt, 2011; Ezcurra et al., 2014; Ezcurra & Butler, 2018). Representatives of this clade, such as non-avian dinosaurs, birds, crocodilians and pterosaurs, have been major components of tetrapod faunas since the Triassic Period, with birds comprising around a third of extant tetrapod diversity (Jetz et al., 2012). Several classic anatomical features, such as the external mandibular fenestrae, closed lower temporal bars, serrated teeth and antorbital fenestrae characterize the archosauriform skull (Gauthier, 1986; Nesbitt, 2011; Ezcurra et al., 2016). However, the evolution of these characters from the typical condition observed in early members of the more inclusive clade Archosauromorpha was, until recently, elusive. The recent description of the archosauromorph *Teyujagua paradoxa* from the Lower Triassic Sanga do Cabral Formation of Brazil, however, started to shed light on this important evolutionary transition. *Teyujagua paradoxa* was recovered by Pinheiro et al. (2016) as the sister-taxon to Archosauriformes, and this species displays several intermediate character conditions that provide new insights into the assembly of the archosauriform skull (Pinheiro et al. 2016).

Teyujagua paradoxa is known only from its holotype, UNIPAMPA 0653, an almost complete skull articulated with lower jaws and cervicals I-IV (Figs 1, 2). This specimen was only briefly described by Pinheiro et al. (2016). Since then, further preparation of UNIPAMPA 0653 has exposed key features of the left side of the skull and cervical vertebrae. In addition, X-ray micro-computed tomography imaging (μCT scans) and 3D modeling of individual bones have revealed anatomical characters which otherwise would be impossible to access. Here we present a complete description of the

holotype of *T. paradoxa*. We also reassess the phylogenetic relationships of *T. paradoxa* using two different phylogenetic frameworks and discuss the early evolution of key characters of archosauriform craniomandibular anatomy.

INSTITUTION ABBREVIATIONS

AMNH, American Museum of Natural History, New York, USA; BP, Evolutionary Studies Institute (formerly Bernard Price Institute for Palaeontological Research), University of the Witwatersrand, Johannesburg, South Africa; CAPPA/UFSM, Centro de Apoio à Pesquisa Paleontológica da Quarta Colônia, São João do Polêsine, Brazil; FMNH, Field Museum of Natural History, Chicago, USA; GMPKU, Geological Museum of Peking University, Beijing, China; ISIR, Indian Statistical Institute Reptiles, Kolkata, India; IVPP, Institute of Vertebrate Paleontology and Paleoanthropology, Beijing, China; MCN, Museu de Ciências Naturais, Fundação Zoobotânica do Rio Grande do Sul, Porto Alegre, Brazil; MCP, Museu de Ciências e Tecnologia da Pontifícia Universidade Católica do Rio Grande do Sul, Porto Alegre, Brazil; MSNM, Museo di Storia Naturale, Milano, Italy; NHMUK, Natural History Museum, London, United Kingdom; NMK, Naturkundemuseum im Ottoneum, Kassel, Germany; NM QR, National Museum, Bloemfontein, South Africa; PIMUZ, Paläontologisches Institut und Museum der Universität Zürich, Zurich, Switzerland; PIN, Borissiak Paleontological Institute of the Russian Academy of Sciences, Moscow, Russia; PVSJ, División de Paleontología de Vertebrados del Museo de Ciencias Naturales y Universidad Nacional de San Juan, San Juan, Argentina; RC, Rubidge Collection, Wellwood, Graaff-Reinet, South Africa; SAM-PK, Iziko South African Museum, Cape Town, South Africa; UA, University of Antananarivo, Antananarivo, Madagascar; UCMP, University of California Museum of Paleontology, Berkeley, CA, USA; UFRGS, Universidade

Federal do Rio Grande do Sul, Porto Alegre, RS, Brazil; ULBRA, Universidade Luterana do Brasil, Canoas, Brazil; UNIPAMPA, Universidade Federal do Pampa, São Gabriel, Brazil; UTGD, School of Earth Sciences, University of Tasmania, Hobart, Tasmania, Australia.

MATERIAL AND METHODS

X-RAY MICROTOMOGRAPHY ANALYSIS (μCT SCAN) AND 3D-MODELING

In order to better access the morphology of skull bones, especially those elements that were not exposed by mechanical preparation, we conducted high-resolution x-ray computed tomography (μCT scanning) of the holotype of *Teyujagua paradoxa* (UNIPAMPA 653) using a Nikon XT H 225 ST X-ray tomography scanner at the School of Earth Sciences, University of Bristol, UK. The scan was set with 224 kV of X-ray energy, 163μA of current and 1.41 s of exposure time. A 0.5 mm tin filter was used and 4x frame averaging was applied (4 frames/projection). To maximize resolution, the specimen was scanned in two adjacent regions of interest, each part taking approximately 5 h to scan. The scan data were reconstructed using CT Pro 3D software, and the two regions of interest were combined using VG Studio Max. This procedure resulted in 3,358 tomographic slices of the specimen, 3,297 of which contain skull/vertebrae data. Unfortunately, limited x-ray penetration of the carbonaceous matrix limited resolution of those bones deeply embedded in rock or surrounded by particularly dense portions of the matrix. Virtual preparation and separation of skull bones through segmentation of individual slices was performed using the software Avizo.

PHYLOGENETIC ANALYSES

The phylogenetic analyses conducted here aimed to test the relationships of *Teyujagua paradoxa* among archosauromorphs. In particular, our aim was to assess the impact of new character state scorings provided by our detailed anatomical description on the phylogenetic position originally recovered by Pinheiro et al. (2016). Additionally, we also wanted to reconstruct the evolution of key characters during the assembly of the archosauriform skull.

We performed two different analyses, using two previously published datasets. First, we updated the scores of *T. paradoxa* in the data matrix of Pinheiro et al. (2016) (Analysis I). This resulted in 65% missing data for *T. paradoxa*, as opposed to 73% missing data in the original data matrix. Although this dataset includes a limited taxon sampling when compared to more recent analyses (e.g. Ezcurra, 2016), we choose to include it for being the original data matrix for which the phylogenetic position of *Teyujagua* was tested (Pinheiro et al., 2016), being relevant to access whether the new scores impacted the original conclusions. The second analysis (Analysis II) was based on the updated scores of *T. paradoxa* in the recent dataset of Butler et al. (2019), which, in turn, represents a modification of the original data matrix of Ezcurra (2016). As the raw dataset of Butler et al. (2019) is an exhaustive assessment of archosauromorph taxa, including a large number of OTUs with a considerable amount of missing data and/or with still unresolved taxonomic issues (see Ezcurra, 2016), we pruned *a priori* 35 terminals, namely: *Dinocephalosaurus*, *Macrocnemus obristi*, *Fuyuanosaurus*, *Pectodens*, *Protanystropheus*, *Trachelosaurus*, *Tanystropheus haasi*, *Eorasaurus*, *Prolacertoides*, '*Archosaurus* holotype', '*Archosaurus* hypodigm', 'Panchet proterosuchid', *Vonhuenia*, *Chasmatosuchus rossicus*, *Chasmatosuchus magnus*, *Chasmatosuchus vjushkovi*, *Koilamasuchus*, *Kalisuchus*, NMQR 3570, *Shansisuchus*

kuyeheensis, *Uralosaurus*, '*Osmolskina* holotype', '*Osmolskina* hypodigm', 'Otter Sandstone archosaur', *Stagonosuchus*, *Dagasuchus*, *Hypselorhachis*, 'Waldhaus poposauroid', *Vysthegdosuchus*, *Bystrowisuchus*, *Bromsgroveia*, 'Moenkopi poposauroid', *Mandasuchus*, *Lutungutali* and *Nyasasaurus*. The resulting dataset comprises 151 taxa and 695 characters. The scoring of *Teyujagua paradoxa* in Butler et al. (2019) used in Analysis II resulted in a proportion of missing data of 58%.

All datasets were edited using the software Mesquite v. 3.51 (Maddison & Maddison, 2018). Heuristic searches were performed in TNT (Tree Analysis Using New Technology) v. 1.5 (Goloboff & Catalano, 2016). We performed a first round of analysis using the New Technology search of TNT (Ratchet and Tree Fusing, 100 hits). This enables the software to continue parsing until the best result (i.e. lowest tree length) is hit 100 times. Following this, we performed a second search using the tree bisection reconnection (TBR) algorithm starting with the trees recovered in the first round of searching.

RESULTS

SYSTEMATIC PALAEONTOLOGY

Diapsida Osborn *sensu* Laurin, 1991

Sauria McCartney, 1802 *sensu* Gauthier et al. 1988

Archosauromorpha Huene, 1946 *sensu* Gauthier et al. 1988

Teyujagua paradoxa Pinheiro et al. 2016

Holotype UNIPAMPA 653, the holotype and, so far, only known specimen of *Teyujagua paradoxa* consists of an almost complete, well preserved skull articulated

with the complete lower jaws, the atlas-axis complex, cervical vertebrae III and IV, and some tiny fragments of cervical vertebra V (Figs 1, 2).

Type horizon and locality UNIPAMPA 653 was recovered from a fine sandstone layer with abundant carbonaceous concretions, about 5 m from the base of 'outcrop 5', Bica São Tomé locality (Da Rosa et al., 2009), Lower Triassic Sanga do Cabral Formation (SCF), Brazil (29°36′ 56″ S, 55°03′ 10″ W). The outcrop is dominated by fine reddish sandstones intercalated with coarse sandstones and intraformational conglomerates, indicating a vast alluvial plain occasionally flooded by shallow braided streams (Zerfass et al., 2003; Da Rosa et al., 2009; Pinheiro et al., 2016; Dias-da-Silva et al., 2017). An Induan–Olenekian age is inferred for SCF based on the presence of the parareptile *Procolophon trigoniceps,* allowing the correlation between SCF and the upper Katberg Formation of the South African Karoo Basin (Dias da Silva et al., 2006, 2017; Botha & Smith, 2006). The type locality of *Teyujagua paradoxa* has already yielded the capitosauroid temnospondyl *Tomeia witecki* (Eltink et al., 2017), still undescribed archosauromorph remains and abundant cranial and postcranial procolophonoid bones, including fairly complete skulls of *P. trigoniceps* (Da Rosa et al., 2009; Dias-da-Silva et al., 2017; Silva-Neves et al., 2018). Tanystropheid archosauromorphs were also reported for other classic SCF localities (Oliveira et al., 2018).

Emended diagnosis Teyujagua paradoxa differs from all other known archosauromorphs on the basis of the following unique combination of characters (autapomorphies indicated by *): large, confluent external nares; external antorbital fenestrae absent; open lower temporal bars; lateral mandibular fenestrae present and positioned beneath the orbits when the lower jaw is occluded*; premaxillae lack anterodorsal processes; premaxillae bear posterodorsally directed palatal processes; anterior maxillary foramina absent; medial antorbital fossae present in maxillae; nasals

are completely dorsal elements; lacrimals are broad and fill the space between the ascending and posterior processes of the maxillae; frontals have a small contribution to orbital rims; posterolateral processes of parietals elevated well above the skull roof; dorsal borders of the supratemporal fenestrae level with the dorsal margins of the orbits; squamosals with elongate ventral processes that reach a point level with the ventral margins of the orbits; wide, anteriorly open quadrate foramen; triangular supraoccipital; splenials exposed in lateral view; surangular shelves present; labiolingually compressed marginal teeth; marginal teeth distally carinated and bearing serrations; pterygoid dentition with a single tooth row on zone T3, zone T2 with two rows and zone T4 present*; strong longitudinal lamina on the lateral surface of the axial centrum*; neural spine of cervical vertebra III with a rounded posterior projection*.

COMPARATIVE DESCRIPTION

Skull

General skull morphology and major openings: The skull is 114.5 mm long, as measured from the tip of the snout to the posterior ends of the quadrates. While the right side of the skull is very well preserved (Fig. 1A), the left side experienced a considerable degree of deformation and abrasion, with the lateral surface of the maxilla obliquely compressed and a dorsomedially displaced left mandibular ramus (Fig. 1B). Partial exposure of the skull prior to collection resulted in considerable damage to the left postorbital bar and anterior left orbital margin. *Teyujagua* had a comparatively short snout, with the preorbital region accounting for about 43% of the total skull length. In dorsal view, the lateral margins of the snout initially diverge in the posterior direction at an angle of about 24° to each other. Close to the anterior margins of the orbits, the skull

abruptly expands laterally, reaching close to its maximum width at the level of the postorbital bar (Fig. 1C). More posteriorly there is a very gentle further expansion until the actual maximum width, located between the squamosals.

The skull and lower jaws present a unique pattern of major openings. The nares are conjoined into a single, enlarged opening that faces dorsally and slightly anteriorly (and is therefore not visible in lateral view) and which is equal in length to 20% of skull length. The conjoined narial opening has a broadly rectangular outline in dorsal view, with a 'W'-shaped posterior margin. There is no antorbital fossa or fenestra on the lateral surface of the skull. The orbits are comparatively large (anteroposterior length is ~17% of skull length) and are located at about the anteroposterior mid length of the skull. They face primarily laterally, but are also visible in dorsal view due to the lateral placement of the jugal with respect to the skull roof. They are subcircular in outline in lateral view. The infratemporal fenestrae are large and have open lower temporal bars along their ventral margins. The main parts of these fenestrae have a trapezoidal outline, being anteroposterior longer at their ventral margins than dorsally. A small posteroventral extension of the infratemporal fenestra occurs beneath the ventral process of the squamosal. The supratemporal fenestrae have chicken-egg-shaped outlines, are broadly separated from one another by the parietals, have vertical margins and are not surrounded by supratemporal fossae. There are also comparatively large, slit-like post-temporal openings present on the occiput, between the posterolateral wings of the parietals and the paroccipital processes.

In the lower jaw, well-developed lateral mandibular fenestrae are present. These openings are unusually anteriorly positioned, being located beneath the orbits when the lower jaw is in occlusion (Fig. 2A, B). They form long, oval slits, with estimated lengths around 20% of total skull length.

Premaxillae: Both premaxillae are preserved in UNIPAMPA 0653 (Fig. 3). They are both essentially complete, although the left premaxilla is partially covered with sediment and small parts are missing at its anterior end. The premaxillae are nearly in articulation, but the left premaxilla has been displaced slightly dorsally and posteriorly, and a very narrow (~1 mm) sediment-infilled gap separates them at the anterior midline.

The main bodies of these bones are anteroventrally inclined at about 20° with respect to the alveolar margins of the maxillae, and they contact each other medially to form a rounded snout in dorsal view (Fig. 3E, F). The anteroventral inclination of the premaxillae observed in UNIPAMPA 0653 resembles the condition in some specimens of *Prolacerta* (e.g. BP/1/471) (Modesto & Sues, 2004). Downturned premaxillae in *Prolacerta*, however, may sometimes be a taphonomic artifact generated by the loose connection between premaxillae and maxillae, and a straighter transition between these bones is suggested by some other specimens (AMNH 9529, UCMP 37151) of this taxon (Spiekman, 2018). The anteroventral inclination of the premaxillae in UNIPAMPA 0653 does not reach the extreme condition often observed in proterosuchid archosauriforms (Ezcurra, 2017). Erythrosuchids display a moderate (*Erythrosuchus africanus*, BP/1/5207) to strong (*Garjainia prima*, PIN 2394/5-1) ventral inclination of the premaxillary alveolar margins, representing an intermediate condition between that observed in UNIPAMPA 0653 and *Proterosuchus* (Gower, 2003; Ezcurra et al., 2019).

The contact between the two counterparts is relatively narrow dorsoventrally. A well-developed and dorsoventrally compressed posterodorsal process forms a considerable posterior extension of each premaxilla (Fig. 3A, B). This process ventrolaterally forms a broad contact with the anterior margin of the maxilla and its dorsomedial surface forms more than half of the lateral margin of the confluent external naris, similar to the condition in the early rhynchosaur *Mesosuchus* (SAM-PK-6536;

Dilkes, 1998) and *Prolacerta* (BP/1/471) (Modesto & Sues, 2004). In *Mesosuchus* and other rhynchosaurs, however, the posterodorsal processes laterally flank the nasals, and contact the prefrontals posteriorly (Ezcurra et al, 2016). UNIPAMPA 0653 also differs from early archosauriforms such as *Proterosuchus* (e.g. RC 846) and *Garjainia* (PIN 2394/5-1), in which the posterodorsal processes usually form the entire lateral margins of the external nares. The posterodorsal processes taper posteriorly and form very small, discrete contacts with the acute anterolateral processes of the nasals close to the mid-length of the external naris (Fig 2C). This condition is unlike most non-archosauriform archosauromorphs. In tanystropheids such as *Tanystropheus* (PIMUZ T 3901), the contacts between the nasals and the premaxillae are located close to the posterior borders of the external nares (Nosotti, 2007), whereas in the allokotosaurian *Azendohsaurus* these bones probably contacted each other posterior to the external nares (Flynn et al., 2010). Moreover, the premaxillae form much broader contacts with the nasals in most other archosauromorphs.

The lateral surfaces of the premaxillae of UNIPAMPA 0653 are convex. A slit-like gap, approximately 5 mm long, is present at the contact between the premaxilla and maxilla on the right side (Fig 3E). It is unclear if this gap is a natural feature or a taphonomic artifact generated by a slight anterior displacement of the premaxilla, which seems to be only loosely connected with the maxilla. Indeed, overlapping joints appear to have been present between premaxillae and maxillae, so that the dorsal margins of the premaxillae stand out above the maxillae in lateral view. Gaps between premaxillae and maxillae are relatively common in archosauromorphs. Among non-archosauriforms, *Azendohsaurus* (FMNH PR 2751) possesses conspicuous grooves on the main bodies of the premaxillae, which are connected to anteriorly-opening maxillary foramina (Flynn et al., 2010). *Mesosuchus* (SAM-PK-5882) has a similar morphology, but also has a

second gap, dorsal to the anterior maxillary foramen and mainly formed by a notch in the maxilla (Dilkes, 1998). Well-developed slit-like gaps are also present in most specimens of *Proterosuchus* (e.g. RC 846). Potentially homologous structures are also present in crownward archosauriforms, such as in erythrosuchids (e.g. *Garjainia*, PIN 2394/5-1), a number of "rauisuchians" (e.g. *Prestosuchus*, ULBRA-PVT-281; Lacerda et al., 2016; Roberto-da-Silva et al., 2016, 2018), some early dinosaurs (e.g. *Herrerasaurus*, PVSJ 407; Sereno and Novas, 1993) and pterosaurs (e.g. *Dorygnathus*, Ösi et al., 2010).

There is no diastema or notch at the transition between the alveolar margins of the premaxillae and the maxillae. Probably as a consequence of the development of confluent external nares, the premaxillae of *Teyujagua* lack anterodorsal (nasal) processes along the midline (Fig. 3B, D). Combined with the gentle transition between the main body and the posterodorsal process, the absence of an anterodorsal process gives the premaxillae a distinct sigmoid shape in lateral view (Fig. 3A). The absence of an anterodorsal process and the consequent confluence of the external nares is an unusual feature in archosauromorphs. Among non-archosauriforms, confluent nares are apparently present in allokotosaurians, such as *Pamelaria*, *Azendohsaurus* and *Shringasaurus* (Sen, 2003; Flynn et al., 2010; Sengupta et al., 2017), and this feature is also a synapomorphy of the extremely specialized rhynchosaurs (Ezcurra et al., 2016). In *Azendohsaurus* (FMNH PR 2751), although the premaxillae lack anterodorsal processes, it is unclear if an internarial bar formed completely by the nasals was present. As such, the condition in *Teyujagua* is more similar to that observed in Rhynchosauria, as early members of this clade, such as *Mesosuchus* (SAM-PK-6536), already presented confluent nares as a consequence both of the absence of the anterodorsal processes of

the premaxillae and of the reduction of the anterior processes of the nasals (Dilkes, 1998).

A very shallow narial fossa is present on the main body of each premaxilla, adjacent to the anterior edge of the confluent external nares. There are no obvious large foramina in this fossa, or elsewhere on the lateral surface of the premaxilla, although poor surface preservation makes it unclear whether smaller nutrient foramina were present. As revealed by CT scans, the palatal surface of the right premaxilla is gently concave, and this bone bears a well-developed and short, posterodorsally directed palatal process (Fig. 3B, C, D). In ventral view, the lateral margin of this process extends anteroposteriorly in a near parasagittal plane, whereas the medial margin extends posterolaterally at an angle of about 32° away from its contact with the opposite premaxilla (Fig. 3C). The palatal process tapers posteriorly to a pointed tip. The presence of a palatal process is an interesting feature of *Teyujagua*, as this is a condition typical of archosauriforms, and is also present in *Prolacerta* and *Boreopricea* (Benton & Allen, 1997; Ezcurra, 2016), both close relatives of the clade. Each premaxilla bears four tooth positions. The alveoli are oval in shape, with their labiolingual axes being longer than their mesiodistal axes (Fig. 3C). Bone lamellae separating successive alveoli are complete between tooth positions two and three and three and four, whereas the first and second alveoli are confluent. In addition, the first alveolus is open medially, as is the case for the posterior margin of the fourth and last premaxillary alveolus.

Maxillae: The maxillae are both completely preserved, although the right element is better preserved and exposed than the left one (Fig. 4). They are broadly triangular in shape and are primarily exposed in lateral view, forming the majority of the lateral surface of the skull anterior to the orbit (Fig. 4E, F). Although they are mainly exposed on the lateral surface, the maxillae also make a modest contribution to the skull table.

Due to the flattening of the snout, the dorsal edges of the maxillae gently curve medially, so that their straight sutures with the nasals can only be seen in dorsal view (Fig. 2C), and the nasals are almost entirely hidden in lateral view. The sutures between the maxillae and the nasals are not parasagittal, but are positioned slightly further medially at their anterior ends than at their posterior ends; as a result, the maxillae form slightly more of the skull table at their anterior ends than they do posteriorly (Fig. 2C). In a highly unusual condition for archosauromorphs, the anterior ends of the maxillae are located well anterior to the anterior ends of the nasals. This feature is only widespread among rhynchosaurs and proterochampsids and is probably a consequence of the confluent nares (despite the fact that, in proterochampsids, the external nares are not confluent).

The lateral surface of the right, better preserved, maxilla is slightly concave dorsoventrally, but there is no sign of an antorbital fossa or fenestra (Fig. 4A). The maxillae bear posterodorsally oriented, tapering ascending processes. While in the left maxilla the ascending process appears to end in a pointed tip, the better-exposed right maxilla bears a small concavity that accommodates a small anterior projection of the prefrontal. Among non-archosauriform archosauromorphs with well-preserved skulls, only *Prolacerta* (e.g. BP/1/471), *Boreopricea* (PIN 3708/1) and the allokotosaurian *Azendohsaurus* (FMNH PR 2751) possess lacrimals that separate the maxillae from the prefrontals (Benton & Allen, 1997; Modesto & Sues, 2004; Flynn et al, 2010).

The posterior (jugal) processes of the maxillae are well developed, comprising approximately half of the total anteroposterior length of these bones (Fig. 4A). The posterior processes are posteriorly overlain dorsally by the anterior (maxillary) processes of the jugals. As revealed by CT scans, the contact surfaces for the jugals are marked by a relatively deep concavity that is laterally delimited by an oblique ridge

(Fig. 4A). Starting close to the contact with the jugal, the posterior process of the right maxilla displays several longitudinal grooves parallel with each other and with the alveolar margin (Fig. 4E). Sometimes these grooves appear to terminate in nutritive foramina anteriorly and fade posteriorly.

The concave rims that separate the ascending and the posterior processes of the maxillae articulate with the lacrimals, which completely fill the gap formed by the confluence of these processes (Fig. 4F). The condition observed in UNIPAMPA 653 resembles that of *Azendohsaurus* (FMNH PR 2751; Flynn et al., 2010), as the common condition in archosauromorphs is that the lacrimals contact only the posterior processes of the maxillae. In Archosauriformes the ascending and posterior processes of the maxillae are usually separated and border anterodorsally the antorbital fenestrae, so that the antorbital openings probably evolved through a posterior retraction of the lacrimals. Anterodorsally, the ascending processes of the maxillae are overlain by the posterodorsal processes of the premaxillae (see above). CT scans reveal that the contact surfaces for the premaxillae bear deep, posteriorly tapering concavities to accommodate the posterodorsal processes of these bones (Fig. 4D). The contact between premaxillae and nasals excludes the maxillae from the margin of the external nares. A contribution of the maxillae to the external nares is moderately common among archosaurs (e.g. pterosaurs, most aetosaurs, some “rauisuchians” and dinosaurs) (Nesbitt, 2011), but it is unusual for early archosauromorphs, one exception being the tanystropheid *Macrocnemus* (e.g. PIMUZ T 4822). The alveolar margins of the maxillae are distinctly straight in lateral view; in ventral view, they curve laterally close to their contacts with jugals (Fig. 4C). The right, completely prepared, maxilla has sixteen tooth positions, located throughout the whole extension of the bone. The lateral surfaces of the maxillae lack anterior maxillary foramina (*sensu* Modesto and Sues, 2004). The absence of

anterior maxillary foramina is usually regarded as synapomorphic for Archosauriformes, and the foramina occur widely among non-archosauriform archosauromorphs.

The medial surfaces of the maxillae, as revealed by CT scans, show deep fossae (here referred to as the 'medial antorbital fossae'), limited posteriorly by the concave contacts with the lacrimals and extending anteriorly as far as the fifth maxillary tooth positions (Fig. 4B). These fossae are arrowhead-shaped, with straight, anteriorly converging ventral and anterodorsal margins. The anterodorsal margins of the medial antorbital fossae extend along the entire height of the ascending processes of the maxillae, and are well-delimited by a distinct ridge. In contrast, the ventral margins of the fossae have rounded rims and extend posteriorly for approximately half the lengths of the posterior maxillary processes. Although the maxillae are comparatively mediolaterally thick, the lateral walls of the medial antorbital fossae are exceptionally thin. Although the presence of medial antorbital fossae might appear to be a unique feature of *Teyujagua*, at least one specimen of *Prolacerta* (BP/1/2675), in which maxillae are exposed in medial view, bears a similar structure (see below). The medial surfaces of the ascending processes bear distinct articulation facets for the nasals, in the shape of a double ridge delimiting a longitudinal groove.

Nasals: The nasals (Fig. 5) are both completely preserved. They are broad and are major elements of the skull table, being restricted to the dorsal surface of the snout (Fig. 2C) and being almost completely hidden in lateral view (a tiny portion of the nasal may be visible in lateral view dorsal to the maxilla-prefrontal suture). Having nasals that are completely dorsal elements is an unusual condition among archosauromorphs, and is most likely a consequence of the flattened snout and the dorsal position of the conjoined nares. However, in other non-archosauriform archosauromorphs with mostly dorsally

positioned nares, such as *Mesosuchus* (SAM-PK-6536) and *Azendohsaurus* (UA-7-20-99-653), the nasals are still exposed in lateral view. The restriction of the nasals to the dorsal surface of the skull, as observed in *Teyujagua*, was independently achieved only by more specialized rhynchosaurs (e.g. *Hyperodapedon*, UFRGS PV0132T; *Teyumbaita*, UFRGS-PV-0232T) and proterochampsians (e.g. *Proterochampsa nodosa*, MCP 1694 PV) (Barberena, 1981; Benton, 1983; Langer & Schultz, 2003; Dilkes & Arcucci, 2012; Trotteyn et al., 2013).

The midline suture between the two nasals is not clearly visible. The nasals form a flat to gently concave external surface. Anteriorly, each nasal bifurcates into two processes, giving the posterior margin of the confluent nares a 'W'-shaped outline in dorsal view (Fig. 2C). The longest process is the lateral one, a very narrow and tapering extension that forms approximately half of the lateral margin of the confluent nares and that contacts the premaxilla anteriorly (Figs 2A, 5A). Anteromedially, each nasal has a short blunt process that is sutured with its counterpart along the midline. This second process is probably homologous to the anterior process of the nasal that contributes to the separation of the external nares in most diapsids. The configuration of both processes of the nasals of *Teyujagua* is very similar to the condition in *Mesosuchus* (SAM-PK-6536), which also has short and blunt medial processes combined with lateral processes that delimit a considerable portion of the external nares. Tanystropheids (e.g. *Tanystropheus*, PIMUZ T 3901; *Macrocnemus*, GMPKU-P-3001) appear to lack lateral processes of the nasals (Nosotti, 2007; Jaquier et al., 2017), and the condition for allokotosaurians seems to be very short lateral processes and long medial processes (e.g. *Azendohsaurus*, UA-7-20-99-653; Flynn et al., 2010). In early archosauriforms, the septum dividing the nares is usually formed by anterodorsal

processes of the premaxillae, with a limited contribution of the medial processes of nasals (e.g. *Proterosuchus*, NMQR 880).

The nasals form straight sutures with the maxillae anterolaterally (see above). Posterolaterally, the nasal-maxilla contact is continuous with that between nasals and prefrontals, but its orientation changes, such that it is more medially placed at its posterior end than at its anterior end (Fig. 2C). As such, the lateral margins of the nasals are convex in dorsal view. At their contacts with the maxillae, the lateral margins of the nasals are deflected ventrally at an angle of about 20° with respect to the skull table. The lateral surfaces of these ventral projections are completely overlapped, and thus hidden, by the maxillae and each one bears a prominent longitudinal crest separating two deep grooves, perfectly matching the double-ridged medial surface of the ascending process of the maxilla (see above) (Fig. 5D). The contact between the nasals and frontals is mostly obliterated by several fractures and considerable compression of the skull table between the orbits and the external nares, but seems to be positioned level with the anterior limits of the orbits, in a similar position to that occurring in the rhynchosaur *Mesosuchus* (SAM-PK-6436) and *Prolacerta* (BP/1/5066).

Lacrimals: The lacrimals (Fig. 6) are preserved on both sides of the skull, although the right one is better preserved. They are triangular elements with no dorsal exposure on the skull roof. These bones completely fill the space between the ascending and posterior processes of the maxillae (Fig. 2A). CT scans reveal that their anterior ends form pointed tips that are laterally covered by the maxillae (Fig. 6A, B). The posterodorsally broad lacrimals of *Teyujagua* differ from most non-archosauriforms. In tanystropheids (e.g. *Tanystropheus*, PIMUZ T 3901), early rhynchosaurs (e.g. *Mesosuchus*, SAM-PK-6536) and *Prolacerta* (BP/1/471, BP/1/3575), the lacrimals are slim, anteroposteriorly elongated elements that contact only the posterior processes of

maxillae. In this respect, *Teyujagua* resembles *Azendohsaurus*, which also has large lacrimals that contact both the posterior and ascending processes of the maxillae (Flynn et al., 2010).

Dorsally, the broad contacts between the lacrimals and prefrontals stand out from the dorsolateral surfaces of the snout as low ridges in front of the orbits. The lateral surface of the right lacrimal is excavated by relatively deep, branched grooves. Posteriorly, the lacrimals gently curve medially to contribute to the anterior border of the orbits. In anterior and posterior view, the lacrimals have a sigmoid shape (Fig. 6E, F). Medially these bones have moderately deep ridges, extending from anterodorsal-to-posteroventral (Fig. 6B). These ridges increase the contact surface between the lacrimals and maxillae. Similar to the condition displayed by tanystropheids (e.g. *Tanystropheus*, PIMUZ T 3901; *Macrocnemus*, PIMUZ T 4822) and rhynchosaurs (*Mesosuchus*, SAM-PK-6536), there are no contacts between the lacrimals and the nasals. This contact, however, is present in *Azendohsaurus* (UA-7-20-99-653), *Boreopricea* (PIN 3708/1), *Prolacerta* (e.g. BP/1/471) and most archosauriforms. The lacrimals contact the jugals at the anteroventral margins of the orbits. The naso-lacrimal duct is evident in both lacrimals as a moderately deep anterodorsally directed groove, somewhat following the outline of the suture between the lacrimal and the main body of the maxilla (Fig. 6A).

Jugals: The jugals are preserved on both sides of the skull (Figs 3, 7). On the left side the ascending process of the jugal is badly abraded (Fig 1B), whereas on the right side most of the posterior process has been lost (Fig. 8). The jugals are triradiate and contact the maxillae anteriorly, the postorbitals dorsally and form the anteroventral and ventral borders of the infratemporal fenestrae posteriorly. Further preparation of the specimen revealed that the anterior process of the jugal contacts the lacrimals at the anteroventral

margin of the orbit (*contra* Pinheiro et al., 2016). In dorsal view, the jugals are flared laterally relative to the maxillae, with a strongly convex lateral surface, and the skull is widest approximately at the level of the jugal-postorbital bar (Fig. 2C). The main bodies of both jugals are ornamented by a series of anteriorly converging longitudinal ridges that extend onto the bases of the posterior processes of the bones (Figs 1A, 8). The anterior (maxillary) processes of the jugals taper in dorsoventral height and form an extensive contact with the posterior processes of the maxillae. The contact between the jugal and the maxilla curves gently dorsally in the anterior direction, and the anterior process of the jugal is similarly curved, delimiting the rounded ventral margin of the orbit (Fig. 8). Though a dorsal curvature of the anterior processes of jugals is widespread among archosauromorphs, the condition observed in *Teyujagua* differs from the pronouncedly curved jugals of tanystropheids (e.g. *Tanystropheus*, PIMUZ T 3901; *Macrocnemus*, PIMUZ T 4822) and *Prolacerta* (BP/1/471), being more similar to early rhynchosaurs such as *Mesosuchus* (SAM-PK-6536) and most archosauriforms.

The ascending processes of the jugals form about half of the postorbital bars, and contact the postorbitals in long sutures that extend diagonally from posterodorsal to anteroventral (Fig. 7G). The better-preserved ascending process of the right jugal has a shallow longitudinal concavity on its lateral surface along its entire length. Although the transition between the ascending process and the anterior process is gently rounded (forming the posteroventral margin of the orbit), the long axes of the two processes are oriented at almost 90 degrees to one another. The ascending processes of the jugals form a smaller contribution to the postorbital bars in non-archosauriforms such as tanystropheids and *Prolacerta* (PB/1/3575), and the condition present in *Teyujagua* is more similar to early rhynchosaurs (e.g. *Mesosuchus,* SAM-PK-6536; *Eohyosaurus*, SAM-PK-K10159; Dilkes, 1998; Butler et al., 2015) and most archosauriforms. In spite

of this, the ascending processes form almost the entire anterior borders of the infratemporal fenestrae in allokotosaurians and most rhynchosaurs.

The posterior process is broken at its base in the right jugal, but is completely preserved on the left side of the skull (Fig. 8). This process tapers posteriorly to form an incomplete lower temporal bar, terminating approximately level with the tip of the ventral process of the squamosal. The dorsal margin of the posterior process is straight, whereas the ventral one is gently convex at the base of the process, and gently concave close to the termination of the process. Most non-archosauriforms have incomplete lower temporal bars, with the notable exception of specialized rhynchosaurs (Ezcurra et al., 2016). In addition, the posterior processes of the jugals fail to contact the quadratojugals in some early archosauriforms that have an almost complete lower temporal bar (e.g. *Proterosuchus fergusi,* SAM-PK-K10603; Ezcurra & Butler, 2015).

Prefrontals: Both prefrontals are preserved as parallelogram-shaped elements, and are mostly restricted to the dorsal surface of the skull but also make a small contribution to the lateral surface, immediately dorsal to the lacrimals (Figs 9C, 10). The prefrontals contact both nasals and frontals medially, while their anterior and anterolateral limits contact, respectively, the ascending processes of the maxillae and the lacrimals. The posterolateral rims of the prefrontals form parts of the anterodorsal orbital margins. The prefrontals form considerable parts of the anterior orbital margins in most archosauromorphs. In tanystropheids (*Macrocnemus*, PIMUZ T 4822; *Tanystropheus*, PIMUZ T 3901) and early rhynchosaurs (*Mesosuchus*, SAM-PK-6536; *Howesia*, SAM-PK-5884), almost the entire anterior margins of the orbits are delimited by the prefrontals, with only small anteroventral contributions from the lacrimals. In *Prolacerta* (BP/1/471) and some early archosauriforms (e.g. *Proterosuchus*, NMQR 1484), about half of the anterior orbital margins are formed by the prefrontals, the other

half being formed by the lacrimals. The contribution of the prefrontals to the orbital margin varies widely within Archosauriformes.

The posterior extensions of the prefrontals fail to contact the postfrontals due to the presence of a small contribution of the frontals to the dorsal margins of the orbits (Fig. 9C). The dorsal surfaces of the prefrontals are ornamented by dense clusters of small shallow pits and low rugosities (Fig. 10). This particular ornamentation pattern is restricted to this bone, and does not spread onto the surrounding elements. Circumorbital ornamentation was reported previously for several archosauromorphs, and the prefrontal ornamentation of UNIPAMPA 653 resembles that illustrated by Flynn et al. (2010) for *Azendohsaurus*.

Frontals: Both frontals are preserved and form the midpart of the skull table, between the orbits (Fig. 9). The exact position of the nasal-frontal suture is uncertain, but it seems most likely to be at a point level with the anterior margin of the orbits. At this point the skull table has been slightly deformed and pushed inwards. Although the posterior contacts with the parietals are also not clear, there is some evidence for interdigitation, suggesting that the suture is a largely straight transverse contact approximately level with the posterior margin of the orbit. In this respect, *Teyujagua* is similar to proterosuchids (e.g. *Proterosuchus*, NMQR 1484) and early rhynchosaurs (*Mesosuchus*, SAM-PK-6536; *Howesia*, SAM-PK-5885; Dilkes, 1995, 1998), as the usual condition among non-archosauriform archosauromorphs is a W-shaped suture, with medial processes of frontals fitting into a concavity formed by the parietals. The anteroposterior length of the frontals is slightly greater than their combined width, and the length of the frontals exceeds that of the nasals. The frontals are not fused to one another, and their dorsal surfaces are mostly flat. Laterally the frontals are bordered anteriorly by the prefrontals and posteriorly by the postfrontals. Unusually, there is only

a very small contribution of the frontals to the dorsal rim of the orbit (Fig. 9C). The frontals form most of the dorsal margins of the orbits in most non-archosauriforms. Among those, only in rhynchosaurs (e.g. *Mesosuchus*, SAM-PK-6536; *Howesia*, SAM-PK-5885; *Teyumbaita*, UFRGS-PV-0232T) is the contribution of the frontals to the dorsal orbital edge limited similarly to the condition in *Teyujagua*, and in some rhynchosaurs (e.g. *Brasinorhynchus*, UFRGS-PV-0168-T) the frontals are completely excluded from the orbital margin (Schultz et al., 2016). In most early archosauriforms (e.g. proterosuchids, erythrosuchids), however, the frontals form only a small part of the orbital margins (e.g. Ezcurra & Butler, 2015; Ezcurra et al., 2019). The extent of frontal contribution to the orbital margin in *Garjainia prima* (PIN 2394/5-1), for instance, is similar to the condition displayed by *Teyujagua*.

The surface of the frontal adjacent to the orbital rim has some fine, striated ornamentation, similar to and continuous with that on the adjacent prefrontal and postfrontal (Fig. 10). The frontals are excluded from the borders of the supratemporal fenestrae by the presence of a contact between the parietals and the postfrontals/postorbitals (Fig. 9C). As the ventral surface of the frontals could not be accessed by CT data, nothing can be said about the olfactory duct and bulbs.

Parietals: The parietals are completely preserved on both sides of the skull (Fig. 9C). The two elements are not fused to each other and show a clear median suture, as is common among non-archosauriform archosauromorphs, with the exception of rhynchosaurs (e.g. Dilkes, 1995; Dilkes, 1998; Montefeltro et al., 2010) and some tanystropheids (e.g. *Macrocnemus fuyuanensis*, GMPKU-P-3001). The contribution of the parietals to the skull table is roughly trapezoidal, and they are perforated at mid-length by a small pineal foramen (Fig. 9A). The foramen is completely enclosed by the parietals, which lack a pineal fossa. The presence of a pineal foramen is the usual

condition for basal archosauromorphs, and the loss of this opening presumably occurred close to the origins of Archosauriformes. *Prolacerta* (BP/1/3574, BP/1/471) still has a well-developed pineal foramen (Modesto & Sues, 2005), while *Proterosuchus* is polymorphic for this feature, with some specimens displaying a vestigial parietal foramen (e.g. NMQR 880, BP/1/3993; Ezcurra & Butler, 2015). An independent loss of the pineal foramen also appears to have occurred within Rhynchosauria, given that *Mesosuchus* (SAM-PK-6536), an early representative of this clade, still displays the plesiomorphic condition of a large pineal opening perforating its fused parietals (Dilkes, 1998).

Although considerably long, the parietals are almost restricted to the postorbital region of the skull, in a morphology that is typical for non-archosauriforms. The parietals form all of the medial borders of the supratemporal fenestrae, but supratemporal fossae are absent. Instead, the parietals show slightly elevated rims bordering the supratemporal fenestrae. The posterolateral processes are plate-like, mostly vertically oriented and elevated well above the main bodies of the parietals. Among non-archosauromorphs, plate-like, subvertical posterolateral processes as displayed by *Teyujagua* are present in allokotosaurians (*Azendohsaurus*, UA-7-20-99-653), basal rhynchosaurs (e.g. *Mesosuchus*, SAM-PK-6536) and *Prolacerta* (BP/1/3575). On the right side of the skull, where the temporal region is completely exposed, the posterolateral process contacts the supratemporal in a region close to the posterolateral corner of the supratemporal fenestra (Fig. 9). The parietals are ornamented by delicate rugosities that converge into the regions close to the transition between the main bodies and the posterolateral processes.

Postfrontal: The postfrontal is completely preserved on the right side, but absent on the left (Figs 9C, 11). Although Pinheiro et al. (2016) identified the contact between the

postfrontal and the postorbital along the lateral edge of the skull table, it is not possible to identify with certainly a suture in this region, although there is a slight break-in-slope and change in the texture of the bone surface. Instead, based on CT data and comparisons with other taxa we identify the suture as extending across the skull roof from the anterior most part of the supratemporal fenestra to the posterodorsal corner of the orbit (Figs 9C, 11C). There is a thin line of sediment in this contact, and the postorbital has been slightly raised up relative to the postfrontal, presumably by post-mortem distortion.

The postfrontal has a trapezoidal outline in dorsal view (Fig. 10). Medially it contacts the frontal along an anteroposteriorly straight suture. As revealed by CT data, the articulation surface with the frontal is dorsoventrally broad and bears a double ridge (Fig. 11B). Posteriorly the postfrontal contacts the parietals and the postorbital, and is excluded from the anterior margin of the supratemporal fenestra, and laterally it contacts the postorbital (Fig. 9C). In a small sample of non-archosauriforms (e.g. *Tanystropheus*, *Jesairosaurus, Trilophosaurus*) the postfrontals contribute to the anterior margins of the supratemporal fenestrae (Ezcurra, 2016).

The postfrontal of UNIPAMPA 653 forms the posterodorsal corner of the orbital margin. Its dorsal surface is ornamented with fine striations, similar to those of the frontal and prefrontal, and these are best developed immediately adjacent to the orbit (Fig. 10). The size of the postfrontal with respect to the postorbital in UNIPAMPA 653 is very similar to the condition in *Prolacerta* (BP/1/471) and *Proterosuchus* (e.g. NMQR 1484). Allokotosaurians (*Azendohsaurus*, UA-7-20-99-653) and the tanystropheid *Macrocnemus* (e.g. PIMUZ T 4822) have postfrontals rivaling the postorbitals in size, whereas rhynchosaurs (e.g. *Mesosuchus*, SAM-PK-6536) show an intermediate condition.

Postorbital: The postorbital is completely preserved on the right side, but only small parts of its internal surface and parts of the posterior process are present on the left side (Fig. 8). The postorbital forms the majority of the gently curved posterior margin of the orbit. It is a triradiate bone, with a medial process that contacts the postfrontal adjacent to the orbit (Fig. 11). The sutural contact with the postfrontal is a straight contact, extending from anterolateral-to-posteromedial, as described above. The posterior process of the postorbital extends along the anterior two thirds of the lateral margin of the supratemporal fenestra. It laterally overlaps the anterior process of the squamosal. The posterior process tapers not far posterior to its contact with the squamosal. This condition is similar to that displayed by *Mesosuchus* (SAM-PK-6536) and tanystropheids (e.g. *Macrocnemus*, PIMUZ T 4822), whereas the condition for most rhynchosaurs, *Azendohsaurus* (UA-7-20-99-653), *Prolacerta* (BP/1/471) and most early archosauriforms is a much longer posterior process, extending close to or beyond the posterior border of the supratemporal opening. The posterior process ends in a broadly rounded tip (proportionately shorter than in *Prolacerta*, BP/1/471) (Fig. 11A, B). The position of the posterior process of the postorbital with respect to the skull roof makes the supratemporal fenestra comparatively tall dorsoventrally, with its dorsal border level with the dorsal margin of the orbit. In this respect, UNIPAMPA 653 resembles the condition observed in most archosauriforms (Ezcurra, 2016). By contrast, the usual condition for non-archosauriform archosauromorphs is a ventrally positioned supratemporal fenestra, with the upper temporal bar level with about mid-height of the orbit (*e.g. Prolacerta,* BP/1/471; tanystropheids) (Modesto & Sues, 1998; Nosotti, 2007; Jaquier et al., 2017). *Mesosuchus* (SAM-PK-6536) and other rhynchosaurs show a similar condition to that present in *Teyujagua* and Archosauriformes, with a dorsally positioned upper temporal bar (Dilkes, 1998).

As supratemporal fossae are absent in UNIPAMPA 653, there are no excavations on the dorsal surface of the posterior process of the postorbital. Although usually absent in early archosauriforms (e.g. *Proterosuchus*), excavated postorbitals contributing to the supratemporal fossae are present in allokotosaurians (Flynn et al, 2010; Ezcurra, 2016) and early rhynchosaurs (e.g. *Mesosuchus*, SAM-PK-6536) (Dilkes, 1998). The ventral process forms a long, gently curved suture with the jugal. This process is broad anteriorly, where a deep longitudinal ridge marks the contact with the jugal medially (Fig. 11B). Posterior to this ridge, the bone becomes a delicate lamina that laterally overlies the dorsal process of the jugal. Similar to *Prolacerta* (BP/1/2675), the ventral process has a weak longitudinal groove that gently curves anteriorly, following the curvature of the process. As is typical among archosauromorphs, the postorbital makes a similar contribution to the jugal to the postorbital bar. The only exception to this is some tanystropheids such as *Macrocnemus* (e.g. PIMUZ T 4822), in which the postorbital forms most of the postorbital bar (Ezcurra, 2016; Jaquier et al., 2017). Ornamentation, in the form of fine striations, is present on the bone adjacent to the postfrontal contact, and extending across the surface of the bone to the border of the supratemporal fenestra (Fig. 10).

Squamosals: The squamosal is partially preserved on both sides of the skull, but is heavily cracked and shattered on each side (Fig. 1A, B). On the left side parts of the anterior process and the entire ventral process are preserved, but the medial process is either missing or covered by sediment, and the posterior process of the bone is missing. On the right side the anterior and medial processes are complete, but the ventral process has largely broken away and the posterior process has shattered and no useful anatomical information can be obtained (Fig 2A). The squamosal forms a small part of the most posterolateral corner of the supratemporal fenestra. The anterior process is

transversely compressed and relatively deep dorsoventrally (Fig. 12A, B), and is laterally overlapped by the posterior process of the postorbital. With respect to the contribution of the anterior process to the lateral border of the supratemporal fenestra, UNIPAMPA 653 is more similar to the typical condition among non-archosauriform archosauromorphs than to that displayed by prolacertids and proterosuchid archosauriforms. In the latter, the anterior process of the squamosal forms more than half of the lateral border of the supratemporal fenestra. Erythrosuchids (*Erythrosuchus*, BP/1/5207; *Garjainia*, PIN 2394/5) share with crownward archosauriforms a limited contribution of squamosals to the lateral border of the supratemporal fenestrae. As revealed by CT scans, the anterior end of the anterior process has a shallow depression to accommodate the posterior process of the postorbital (Fig 12A). Posteriorly, the transition between the anterior and the ventral processes is very gentle, giving the infratemporal fenestra a rounded posterodorsal border, in a very similar condition to that present in proterosuchid archosauriforms (e.g. *Proterosuchus*, NMQR 1484). With some isolated exceptions (e.g. *Protorosaurus*, NMK S 180), the usual condition among non-archosauriform archosauromorphs is a supratemporal fenestra with squared posterodorsal borders. The medial process is short and triangular, and contacts the supratemporal medially, forming only a short part of the posterior border of the supratemporal bar. The ventral process is elongate, and extends nearly directly ventrally, reaching a point level with the ventral margin of the orbit. This is an unusual condition among non-archosauriform archosauromorphs, and occurs only in hyperodapedontine rhynchosaurs (e.g. *Teyumbaita,* UFRGS-PV-0232T). The ventral process is anteroposteriorly broad (similar to *Proterosuchus*, NMQR 1484), with a gently convex anterior margin, and terminates ventrally in a broadly rounded tip. Medially, the ventral process shows a dorsoventrally oriented ridge (Fig 12B), posterior

to which the head of the quadrate is accommodated. Although only well preserved on the right side, some fine surface ornamentation is present on the lateral surface of the main body of the squamosal.

Supratemporal: The supratemporal is preserved on both left and right sides, although the right element is better preserved (Fig. 9C). The supratemporal separates the squamosal from the posterolateral wing of the parietal, and makes a small contribution to the posterior border of the supratemporal fenestra. It also forms part of the dorsolateral border of the post-temporal fenestra (Fig. 14) (see below). The supratemporal is a narrow, rod-like element, with a long axis that extends from anteromedial to posterolateral. The bone is flexed along this long axis so that the part adjacent to the supratemporal fenestra is set more dorsally than the more posterolateral part of the bone. In posterior view it forms a slightly interdigitating suture with the posterolateral wing of the parietal (Fig. 14). Among non-archosauriform archosauromorphs, supratemporals are present in rhynchosaurs and prolacertids (Ezcurra, 2016). In archosauriforms, these bones were only reported for early members of the clade (e.g. *Proterosuchus*, NMQR 1484). The slender nature of the supratemporals of *Teyujagua* is similar to the condition displayed, for instance, by prolacertids (e.g. *Prolacerta*, BP/1/471).

Quadrate: The quadrate is a robust element with a complex morphology (Fig. 13). The left quadrate is completely preserved, but its right counterpart is missing except for some scattered fragments that probably belong to this bone (Fig. 2A). The dorsal part of the posterior margin of the quadrate is subvertical. Level with the ventral limit of the squamosal, the quadrate bends posteriorly, so that the posterior margin of the ventral part of the bone forms an angle of 138° with the posterior margin of the dorsal part of the bone (Fig. 2B). Ventral to this, the posterior margin of the quadrate becomes gently

convex, similar to the condition in *Prolacerta* (BP/1/3575). Although the quadrates of allokotosaurians (e.g. *Azendohsaurus*, UA-7-20-99-653) also have posterior convexities at their ventral ends, in these taxa this bone has a subvertical orientation. Subvertical quadrates are also displayed by some specimens *Proterosuchus* (e.g. NMQR 1484). The quadrate of UNIPAMPA 653 has a broad squamosal contact, articulating somewhat loosely with the whole posterior margin of the ventral process of the squamosal. The quadrate head is overlain by a small posterodorsal extension of the squamosal, but the entire extension of the quadrate, including its head, is widely exposed in lateral view (Fig. 13). The dorsal articulation with the squamosal is a blunt convexity, but does not bend posteriorly, unlike the hook-shaped quadrate head of allokotosaurians (e.g. *Azendohsaurus*, UA-7-20-99-653; *Shringasaurus*, ISIR 820; Flynn et al. 2010; Ezcurra, 2016; Sengupta et al. 2017).

The anterior margin of the quadrate is excavated at its mid-length to form a wide, anteriorly open, quadrate foramen, similar to the one displayed by the archosauriform *Sarmatosuchus* (PIN 2865/68-3; Ezcurra, 2016: fig. 24) (Fig. 13). The ectocondyle is strongly laterally projected, but the entocondyle, as well as the medial pterygoid flange, are still embedded in matrix and limited X-ray penetration hindered their examination. Most interestingly, the quadrate apparently lacks articulation facets for the quadratojugals. This later bone, not preserved in UNIPAMPA 0653, was either very reduced or completely lost in *Teyujagua*, which is a highly unusual condition in Archosauromorpha, apparently only mirrored by *Tanystropheus* (Nosotti, 2007; Ezcurra, 2016). In addition to the absence of quadratojugal contacts on the quadrate of UNIPAMPA 0653, the loss of quadratojugals in *Teyujagua* is supported by the fact that this bone is not preserved on either side of the skull, even though the degree of articulation of the holotype allowed the preservation of small structures, such as atlantal

elements. The absence of quadratojugals in *Teyujagua,* however, can only be confirmed by the discovery of further specimens.

Occiput: A considerable part of the occiput of UNIPAMPA 653 (Fig. 14) is hidden by the atlas/axis complex. Among the exposed elements, the posterolateral processes of the parietals have a wide contribution to the occipital region in the shape of their plate-like posterior surfaces. The contribution of the parietals to the occiput is greater in UNIPAMPA 653 than it is in *Prolacerta* (BP/1/3575) or *Proterosuchus* (NMQR 1484), and is more similar to the condition displayed by *Erythrosuchus* (BP/1/4680; Gower, 2003). Although having a wide contribution of parietals to the occipital surface, *Azendohsaurus* (UA-7-20-99-653) shows much deeper parietal plates than UNIPAMPA 653 (Flynn et al. 2010). The parietals apparently contact each other at the midline, with no evidence for the presence of postparietals. Although postparietals are absent in archosaurs and proterochampsids, they are widely spread among early archosauriforms (Ezcurra, 2016), and are also present in the non-archosauriform *Tasmaniosaurus* (UTGD 54655; Ezcurra, 2014). Laterally, the parietals articulate with the supratemporals.

The supraoccipital is a triangular, anteroposteriorly sloping bone, with its apex almost contacting the dorsal surface of the parietals. A triangular supraoccipital is also present in *Azendohsaurus* (UA-7-20-99-653), while the condition for most archosauromorphs is a rounded, plate-like bone. The ventral margin of the supraoccipital dorsally limits a relatively large foramen magnum. The occipital condyle is obscured by the anterior elements of the cervical series. The left opistothic is represented by its anteroposteriorly flattened paroccipital process, which is posterolaterally deflected from the anteroposterior axis of the skull and ventrolaterally oriented in posterior view. Ventrally-deflected paroccipital processes are also known for

Prolacerta (BP/1/3575) and *Azendohsaurus* (UA-7-20-99-653). In *Proterosuchus* (e.g. NMQR 1484), *Garjainia* (PIN 2394/5-1) and most rhynchosaurs (e.g. *Teyumbaita*, UFRGS-PV-0232T), however, the paroccipital process is mostly horizontally oriented. The distal end of the paroccipital process is broader than its contact with the supraoccipital, and apparently does not contact the parietals or supratemporals, although this may reflect a slight posterior displacement of the paroccipital process. The post-temporal fenestra, which is only visible on the left side, is a large, slit-like aperture, ventrally bordered by the paroccipital process, dorsally by the parietal, and dorsolaterally by the supratemporal (Fig. 14). The post-temporal fenestra of UNIPAMPA 653 differs both from the extremely dorsoventrally constricted condition present in *Proterosuchus* (NMQR 1484) and *Erythrosuchus* (BP/1/4680) (Gower, 2003), and the rounded opening of allokotosaurians with known skulls (e.g. UA-7-20-99-653). Rhynchosaurs display a trend towards developing exceptionally wide post-temporal fenestra, but this is seemingly not the case for the early representatives of the clade (e.g. *Mesosuchus*; Dilkes, 1998). The lack of contact between the paroccipital process and parietals/supratemporals means that the post-temporal fenestra is open laterally as preserved.

Lower jaw

General morphology: The lower jaw (Fig. 15) is a comparatively slender element anteriorly, especially throughout the length of the dentary. Ventral to the orbits, however, the lower jaw expands dorsoventrally, becoming much deeper. The two mandibular rami run parallel and almost contacting each other until close to the sixth maxillary tooth position, where they start to diverge, following the pronounced lateral expansion of the skull. The mandibular symphysis seems, therefore, to be weak and restricted to the anteriormost portion of the dentaries (Fig. 15A, B). The external

mandibular fenestrae are slit-like openings located ventral to the orbits, being mostly bordered by surangulars (posterodorsally) and angulars (anteroventrally), with a small anterior contribution of the dentaries (Fig. 15D). The anterior position of the mandibular fenestrae is unusual. Among most archosauriforms, including early representatives of the clade, these openings are posteriorly displaced, with their anterior borders ending level with the mid length of the orbits. In some specimens of *Proterosuchus* (e.g. RC 846), the external mandibular fenestrae are reduced to small ellipsoid openings ending posterior to the anterior borders of the infratemporal fenestrae. In addition, the contribution of the dentary to the anterior border of the mandibular fenestra is more extensive in most early archosauriforms, such as *Proterosuchus* (e.g. NMQR 1484), *Erythrosuchus* (BP/1/5207), *Garjainia* (PIN 2394/5-8) and *Euparkeria* (SAM-PK-5867) (Ewer, 1965; Gower, 2003; Ezcurra et al., 2019). As the lower jaw was preserved in occlusion, most of its dorsal and medial surfaces are still covered by cranial bones, and rock matrix, but were partly accessed by CT scans (Fig. 15A-C). Unfortunately, poor X-ray penetration in the rock matrix that embeds the posterior part of the medial surface of the lower jaw prevented access to the morphology of the coronoid and prearticular.

Dentaries: Both dentaries are preserved, but their alveolar surfaces are still hidden by matrix. They are comparatively short, slender bones, contributing to less than half of the anteroposterior extension of the lower jaw, in contrast to the anteroposteriorly long dentaries displayed by proterosuchids, *Erythrosuchus* (BP/1/5207), *Garjainia* (PIN 2394/5-8) and *Euparkeria* (SAM-PK-5867). *Prolacerta* (BP/1/471) shows a condition somewhat intermediate between UNIPAMPA 653 and these latter species, whereas *Mesosuchus* (SAM-PK-6536) shows short dentaries in a condition more similar that present in *Teyujagua*. The two dentaries meet close to their anterior end, forming a weak symphysis. Externally, the posteroventral borders of the

dentaries curve dorsally to accommodate the splenials, but this upward bending is revealed to be more abrupt under CT imaging, indicating that the splenials partially cover the dentaries laterally (Fig. 15A, C). The tapering posterior ends of the dentaries make small contributions to the anterior borders of the external mandibular fenestrae (Fig. 15D). The dentaries of UNIPAMPA 553 lack posterocentral or posteroventral processes, and their posterior ends are very similar to the condition observed in *Prolacerta* (e.g. BP/1/471). The presence of a posterocentral process is widespread among early archosauriforms, whereas a posteroventral process is present in erythrosuchids and some crownward clades (Ezcurra, 2016). As revealed by CT images, the right dentary bears sixteen tooth positions (Fig. 15A-C), in contrast to the twenty alveoli displayed by the upper jaws (combined count for premaxilla and maxilla). As a result, the dentary tooth rows end well anterior to the maxillary ones, in a position close to the 11th maxillary alveolus. The dentary count of UNIPAMPA 653 is low in comparison to *Prolacerta* and *Proterosuchus,* being more similar to erythrosuchids and euparkeriids, among others (Gower, 2003; Modesto & Sues, 2004; Ezcurra, 2016, Ezcurra et al., 2019).

Splenials: The splenials are mostly medial components of the mandibular rami. They are anteroposteriorly long, extending from about the posterior border of the external mandibular fenestrae until close to the anterior end of the lower jaw. Throughout their whole extension, the splenials form most of the ventral surfaces of both mandibular rami, gently giving way to the dentaries anteriorly. The contribution of the splenials to the symphysis is unclear. The splenials are exposed in lateral view, ventral to the contact between the angular and the dentary, filling the space left by the gentle dorsal curvatures of these bones (Fig. 15D). Although the splenials are major components of the lower jaw of most archosauromorphs, the lateral exposure of these bones is an

unusual feature for this clade. One exception is the tanystropheid *Macrocnemus* (PIMUZ T 4822, GMPKU-P-3001), which has a wide exposure of the splenials on the lateral surfaces of the mandibular rami, surpassing the condition displayed by UNIPAMPA 653. The splenials also seem to have a limited lateral exposure in the lower jaws of the early rhynchosaur *Mesosuchus* (SAM-PK-5882), and this is also widespread among several other rhynchosaurs (e.g. *Rhynchosaurus*, NHMUK PV R1236; *Teyumbaita*, UFRGS-PV-0232T; *Hyperodapedon*, UFRGS-PV-0132T). *Prolacerta* (e.g. BP/1/471), *Proterosuchus* (e.g. NMQR 1484) and *Euparkeria* (SAM-PK-5867) share the usual condition for Archosauromorpha, in which the splenials are restricted to the medial surfaces of the lower jaw. Among erythrosuchids, at least *Garjainia prima* (PIN 2394/5-8) displays a modest contribution of splenials to the lateral surface of the mandible. In archosauriforms, lateral exposure of splenials is also present in phytosaurs (e.g. *Machaeroprosopus*, AMNH 3060) and proterochampsians (e.g. *Proterochampsa barrionuevoi*, PVSJ 77) (Colbert, 1947; Dilkes & Arcucci, 2012; Ezcurra, 2016).

Angulars: The angulars are long and narrow, having wide lateral exposures on the posterior halves of the mandibular rami (Fig. 15D). These bones apparently make small contributions to the retroarticular processes at their posterior ends, gradually expanding dorsoventrally to reach their widest portion ventral to the infratemporal fenestrae. Anterior to this, the angulars narrow again to form a long anterodorsally-directed process that ventrally border the external mandibular fenestrae, gently ascending and contacting the dentaries anteriorly while laterally overlapping the splenials. This gives the dorsal margins of the angulars a sigmoid outline, and this is a widespread condition among archosauromorphs, being common in archosaurs (e.g. *Prestosuchus*, UFRGS-PV-0629-T; *Decuriasuchus*, MCN-PV10.105a; França et al.,

2013; Mastrantonio et al., 2019) and non-archosaurian archosauriforms (e.g. *Garjainia,* PIN 2394/5-8; *Proterosuchus*, RC 846), and also present in a small sample of non-archosauriform archosauromorphs (e.g. *Prolacerta*, BP/1/471). In *Teyujagua* and archosauriforms, where an external mandibular fenestra is present, the slender, upward-directed anterior ramus shapes the round ventral border of this opening. The participation of the angulars to the medial surfaces of the mandibular rami is still obscured and could not be accessed by CT data.

Surangulars: The surangulars are large bones, composing most of the external posterior halves of the mandibular rami and with their maximum dorsoventral depth level with the postorbital bars (Fig. 15D). Anterior to this, the anteroventral margins of the surangulars gently bend dorsally, composing the entire posterodorsal margins of the mandibular fenestrae. The dorsal margins of the surangulars are slightly convex. Just ventral to the dorsal margins, the lateral surfaces of the surangulars possess step-like anteroposterior shelves that probably accommodated the posterior rami of the jugals. The surangular shelves are well-developed and display nearly straight lateral edges. The presence of surangular shelves is an interesting character of UNIPAMPA 0653, as this structure is almost completely absent in non-archosauriforms, with the exception of the low ridges observed in the surangulars of most rhynchosaurs (Ezcurra, 2016, character 286). Ridged surangulars or well-developed surangular shelves is, thus, a typical feature of Archosauriformes, and the condition in UNIPAMPA 0653 is similar to that in *Euparkeria* (SAM-PK-5867). Posterior to their maximum depth, the ventral margins of the surangulars also curve gently dorsally, to accommodate the main bodies of the angulars. Because the angulars deepen posteriorly, the ventral borders of the surangulars are not entirely convex, having rather a sigmoid shape, in a similar condition to *Prolacerta* (BP/1/471) and *Proterosuchus* (RC 846). As the articulars are displaced

medially from the lateral surfaces of the lower jaw, the surangulars apparently make only limited contributions to the retroarticular processes. A small, posteriorly-directed foramen pierces the lateral surface of the posterior end of the right surangular. Posterior surangular foramina are present in *Azendohsaurus* (FMNH PR 2751), *Eohyosaurus* (SAM-PK-K10159), *Prolacerta* (e.g. BP/1/3575) and a wide range of taxa within Archosauriformes (Ezcurra, 2016, character 289). Poor preservation, however, hinders the recognition of this same structure on the left surangular.

Articulars: The articulars are preserved on both sides of the skull, but the left element is broken and medially displaced. The main feature of the articulars is the presence of very well-developed retroarticular processes, with the right, better preserved one, extending approximately 8 mm posterior to the glenoid fossa (Fig. 15D). The anterior part of the right retroarticular process follows the outline of the ventral margin of the angular. Posterior to this, it develops a dorsomedially directed hook-shaped extension which is medially displaced from the lateral margin of the main body of the articular. Well-developed, upturned retroarticular processes are widely distributed among archosauromorphs, and the condition displayed by UNIPAMPA 0653 resembles that in *Proterosuchus* (RC 846; Ezcurra & Butler, 2015) and *Euparkeria* (SAM-PK-5867; Ewer, 1965). By contrast, erythrosuchids (*Garjainia*, PIN 2394/5-8), *Mesosuchus* (Dilkes, 1998), *Prolacerta* (BP/1/471) and crownward archosauriforms have rather blunt retroarticular processes. The medial surface of the right articular is still embedded in matrix. The left articular apparently lacks a medial foramen, although poor preservation complicates assessment of this character. While absent in most early archosauromorphs, a medial articular foramen is typical of archosauriforms (Ezcurra, 2016, character 294).

Dentition

Marginal dentition Only the marginal dentition of the right premaxilla and maxilla were completely exposed by preparation (Fig. 16C). A few replacement teeth are visible in CT images. Some posterior teeth of the left maxilla are exposed (Fig. 16B), whereas the anterior teeth (as well as the left premaxillary teeth) remain embedded in matrix. The dentary dentition is only accessible through CT data (Fig.15A-C).

Both premaxillae bear four teeth, whereas the maxillae bear sixteen teeth each (Fig. 17A, C, D). Among non-archosauriforms, the premaxillary tooth count present in UNIPAMPA 0653 is only mirrored by the allokotosaurians *Azendohsaurus* (FMNH PR 2751), *Shringasaurus* (ISIR 793) and *Pamelaria* (ISIR 316/1) (Sen, 2003; Flynn et al., 2010; Sengupta et al., 2017). With the exception of *Mesosuchus* (two premaxillary teeth SAM-PK-5882; Dilkes, 1998), *Protorosaurus* (three premaxillary teeth; NMK S 180; Gottman-Quesada & Sander, 2009) and derived rhynchosaurs, all other non-archosauriform archosauromorphs display five or more premaxillae teeth, and the same is true for early archosauriforms (Ezcurra, 2016). The maxillary tooth count present in UNIPAMPA 0653 is also low when compared to most non-archosauriform archosauromorphs and early archosauriforms. The maxillae of *Prolacerta* (BP/1/471), for example, bear up to 25 tooth positions (Modesto & Sues, 2004), and a high maxillary tooth count is also reported for *Proterosuchus*, reaching more than 30 positions in larger specimens (e.g. RC 846; Ezcurra & Butler, 2015).

All the marginal teeth display typical ziphodont morphologies, with sharp, distally curved crowns (Fig. 16). Most of the teeth are labiolingually compressed, the only exception being the anterior most premaxillary teeth, which are circular in cross section. Labiolingual compression of the marginal dentition is typical of archosauriforms. Among early, non-archosauriform archosauromorphs, labiolingually compressed teeth seem only to be present in azendohsaurids (e.g. *Azendohsaurus*, UA

8-29-97-160), *Tasmaniosaurus* and *Prolacerta* (e.g. BP/1/2675) (Ezcurra, 2015, 2016). The marginal dentition of azendohsaurids, however, displays characteristic adaptations for herbivory, such as leaf-shaped expanded crowns and coarse serrations (Flynn et al., 2010, Sengupta et al., 2017).

The premaxillary teeth increase in size distally, with the most mesial tooth pair having short, anteriorly procumbent, crowns. The anterior maxillary teeth are the largest, and the maxillary teeth decrease in size distally (Fig. 16C). The second and fourth maxillary tooth positions on the right side, as well as the first and fourth positions on the left side, are occupied by small replacement teeth. The marginal teeth are distally carinated, but their mesial margins are blunt. When visible, the tooth carinae bear very fine serrations, with approximately ten denticles per millimeter (Fig. 16B). Serrated teeth were, prior to the initial description of *Teyujagua*, considered unique to Archosauriformes (e.g. Nesbitt, 2011; Ezcurra et al., 2014). However, aside from *Teyujagua*, serrated teeth are present in *Azendohsaurus* (UA 8-29-97-160), and were also reported for *Pamelaria* (Ezcurra, 2016, character 304) and *Shringasaurus* (Sengupta et al., 2017). The coarse serrations of the teeth of *Azendohsaurus*, however, strongly differ from the minute denticles displayed by UNIPAPA 0653. The presence of serrations on the distal tooth margin alone is also characteristic of proterosuchid archosauriforms (Ezcurra, 2016).

Although Pinheiro et al. (2016) recognized thecodont tooth implantation for the marginal teeth of UNIPAMPA 653, cross sections of alveoli made with CT data show that tooth roots are ankylosed to the surrounding bone, indicating an ankylothecodont implantation (Fig. 16A). Considering the phylogenetic position of *Teyujagua* among early archosauromorphs (Pinheiro et al., 2016; see below), an ankylothecodont tooth implantation is expected. A fully thecodont dentition is displayed by some

erythrosuchids (e.g. *Garjainia prima*, PIN 2394/5), *Erythrosuchus* (BP/1/2529) and crownward archosauriforms, whereas ankylothecodont dentition is observed in allokotosaurians, rhynchosaurs, *Prolacerta* and the earliest archosauriforms (Ezcurra, 2016; Ezcurra et al., 2019).

Although still enclosed in matrix, dentary dentition was accessed by CT scans (Fig. 15A-C). The better preserved right dentary bears sixteen alveoli, a low tooth count when compared to most non-archosauriform archosauromorphs and early archosauriforms. Early rhynchosaurs, such as *Howesia* (SAM-PK-5884) and *Mesosuchus* (SAM-PK-5882) had dentaries with multiple rows of numerous blunt teeth (Dilkes, 1995, 1998), and the tanystropheid *Macrocnemus* (e.g. GMPKU-P-3001) could bear up to 40 small conical teeth on each dentary. Similarly, dentary tooth count is comparatively high in *Prolacerta* (e.g. BP/1/471), and *Proterosuchus* (RC 846), whose dentaries had room for up to 30 teeth. Dentary teeth are apparently similar to the maxillary ones but have more circular cross-sections. The dentary tooth row ends posteriorly well anterior to the posterior end of the maxillary series – the posterior most dentary tooth is level with the 11th maxillary teeth. Although the dentary teeth bear distal carinae, CT scans do not allow the recognition of possible serrations.

Palatal dentition Although still hidden by matrix, the palate of UNIPAMPA 0653, as recovered by CT scans, shows an extensive presence of teeth (Fig. 17). Limited X-ray penetration hindered the delimitation of palatal bones. However, the palatal dentition is apparently associated with the pterygoids, palatines and vomers. The pterygoid dentition consists of three distinct zones (Fig. 17B). One of these, tooth zone T4 of Welman (1998) extends through the medial border of the palatal ramus. Although tooth zone T4 comprises small, regularly spaced, blunt teeth on the left pterygoid, it shows well developed fang-like teeth on the right side. On both sides, the apicobasal axes of

T4 tooth crowns are medially directed. The presence of tooth zone T4 in UNIPAMPA 0653 is remarkable, as a row of teeth on the medial surface of the palatal process of the pterygoid is restricted to early archosauriforms (e.g. *Proterosuchus*, NMQR 1484) and closely-related taxa, such as *Prolacerta* (e.g. BP/1/2675), *Boreopricea* and *Tasmaniosaurus* (UTGD 54655) (Ezcurra, 2016).

Tooth zone T3 is composed of a single row of small teeth extending throughout the ventral surface of the pterygoid. A single tooth row on zone T3 is uncommon among early archosauromorphs, being thus far only reported for tanystropheids (Ezcurra, 2016, character 197). Posteriorly, the T3 row begins in a region close to the presumed contact with the ectopterygoid, extending through the palatal ramus. T3 teeth are rounded and blunt posteriorly, but gradually become slightly bigger and pointed towards the anterior end of the palatal ramus. Tooth zone T2 consists of two posteriorly converging rows of considerably developed pointed teeth, the medial one apparently being continuous with the palatine dentition. Due to poor X-ray penetration, tooth zone T2 can be consistently identified only on the left pterygoid. The disposition of ventral pterygoid teeth into two distinct fields (T2 and T3) is characteristic of early archosauromorphs, observable, for instance, in *Mesosuchus* (SAM-PK-6536), *Macrocnemus* (PIMUZ T 1559), *Prolacerta* (BP/1/5066) and *Proterosuchus* (NMQR 1484) (Ezcurra, 2016). However, the presence of two tooth rows on field T2 was, among archosauromorphs, only reported for *Macrocnemus* and *Howesia* (Dilkes, 1995; Ezcurra, 2016). Teeth corresponding to tooth zone T1 of Welman (1998), which would be concentrated on the posterior border of the palatine process of the pterygoid, are apparently absent in UNIPAMPA 0653. Among non-archosauriform archosauromorphs, tooth zone T1 is absent in *Jesairosaurus*, tanystropheids and rhynchosaurs (Ezcurra, 2016, character 202).

The combination of i) a single tooth row on zone T3; ii) presence of zone T4; iii) zone T2 composed by two tooth rows and iv) absence of zone T1 is unique among Archosauromorpha, making the pterygoid of UNIPAMPA 0653 highly diagnostic.

Anterolaterally to pterygoid tooth zone T2, the palatal teeth abruptly change in shape from relatively tall and pointed to short and blunt. In addition, the teeth become roughly oriented into two poorly defined anteromedially directed rows (Fig. 17B: 'pld'). This change in morphology probably marks the transition between the pterygoid and the palatine, and the blunt teeth are probably associated with this latter bone. The presence of teeth on the palatine is plesiomorphic for diapsids, being the usual condition among archosauromorphs. Exceptions to this include erythrosuchids, most rhynchosaurs, *Prolacertoides* (IVPP V3233), *Trilophosaurus*, and several clades of crownward archosauriforms (Ezcurra, 2016). The vomerine dentition is oriented as a single row of irregularly spaced fang-like teeth with medially oriented apicobasal axes (Fig. 17A). Vomerine teeth are absent in specialized rhynchosaurs and *Prolacertoides*, whereas *Pamelaria* and *Prolacerta* show multiple rows of teeth on the vomer (Sen, 2003; Ezcurra, 2016, character 187).

Cervical vertebrae

General remarks: The atlas-axis and cervical vertebrae III and IV are completely preserved and lie adjacent to the occiput (Figs 2C, 18). In addition, some very small fragments of cervical vertebra V can be seen in articulation with the fourth element. Although close to natural position, the cervicals are rotated along their main axis, so that their left lateral surfaces are mainly exposed in dorsal view of the specimen. Preparation exposed the left side of the vertebrae, but the right surface is still embedded in the hard, mainly calcium carbonate concretion. As bone density in this particular part of the specimen is exceedingly similar to matrix density, our attempts to reconstruct the

overall surface of vertebrae based on CT scan images failed. At least on the left side, cervical ribs are still in articulation (Fig. 18).

Atlas: At least two atlantal elements lie in close association with the axis and are exposed on the left side of the cervical series (Fig. 18). The dorsal one is here identified as the atlas neural arch. It is a slender bone in lateral view, thicker ventrally and gradually tapering in the dorsal direction, where it curves anteriorly, somewhat following an anterior overhang of the axial neural spine. As preserved, the atlantal neural arch does not present a posterior wing-like expansion to articulate with the axis, as displayed, for example, by *Azendohsaurus* (UA 7-20-99-653; Nesbitt et al., 2015). Additionally, there is a ventral, wedge-shaped element, positioned at the same level as the axis centrum. This small bone is consistent in morphology with a crescent-shaped intercentrum exposed in lateral view, and is here identified as the atlantal intercentrum.

Axis: The axis is a robust element, with a strong neural spine shaped as a wide plate (Fig. 18). Anteriorly and in close association with the axis, there is an additional wedge-shaped bone with a tapering posteroventral projection. This bone is here identified as the axial intercentrum, and the posteroventral projection may correspond to the axial parapophysis. As the anterodorsal part of this bone is still obscured by matrix and atlantal elements, the presence of a fused odontoid process could not be confirmed.

The axial neural spine is longer than tall. It differs from the comparatively low axial neural spines of tanystropheids (e.g. *Tanystropheus*, MSNM BES SC 265; Nosotti, 2007) and *Prolacerta* (Camp, 1945; Ezcurra, 2016). Although mainly rectilinear, its dorsal surface is notched close to the mid length of the neural spine, which may be a taphonomic artifact. Excluding this notch, the neural spine maintains a similar height throughout its anteroposterior extension, differing from the anterodorsally expanded axial neural spine of tanystropheids (e.g. *Tanystropheus*, MSNM BES SC 265). The

anterodorsal corner of the axial neural spine is rounded, so that the transition from the dorsal to the anterior surface is more or less gentle. The neural spine has a distinct anterior overhang, as its outline abruptly curves posteroventrally, shaping a strong concavity. In the way the elements are disposed, this anterior concavity accommodates the atlantal neural arch. In this respect, the axial neural spine of UNIPAMPA 653 is somewhat similar to that in *Azendohsaurus* (FMNH PR 3823). In this latter taxon, however, the dorsal edge of the neural spine increases in height posteriorly (Nesbitt et al. 2015). The axial neural spine of *Prolacerta* maintains its height throughout its extension, but its anterior overhang tapers to form an acute projection (Camp, 1945).

The dorsal surface of the axial neural spine thickens posteriorly, forming a swollen posterodorsal corner. In addition to this swelling, the dorsal surface of the neural spine is slightly transversely expanded throughout its whole extension. In the ventral direction, the neural spine widens to form the postzygapophysis. The postzygapophysis articular facet is horizontally oriented, almost parallel to the dorsal surface of the neural spine. There is no epipophysis, whereas this structure is present in the axis of *Azendohsaurus* (FMNH PR 3823) and, apparently, *Tanystropheus* (MSNM BES SC 265). Similar to UNIPAMPA 0653, epipophyses are absent on the axis of *Prolacerta* (Camp, 1945) and early archosauriforms (e.g. *Proterosuchus*, NMQR 1484; *Garjainia*, PIN 2394/5-10). A small prezygapophysis articulates with the atlantal neural arch. Posteriorly to the prezygapophysis, there is a low lamina that fades long before the mid length of the neural arch, not forming an interzygapophyseal lamina.

The centrum is anteroposteriorly short when compared to *Azendohsaurus* (FMNH PR 3823), *Tanystropheus* (MSNM BES SC 265) and *Prolacerta* (Camp, 1945), being more or less compatible with *Proterosuchus* (NMQR 1484). Close to its anterior limit, it bears a ventrolaterally directed diapophysis, posterior to which a strong lamina

extends throughout its entire length, reaching the articulation facet with the third cervical vertebra. Ventral to this lamina, the centrum is laterally compressed. The way the vertebrae are preserved precludes the identification of a possible ventral keel. The posterior articulation facet of the axis is positioned slightly ventral to the anterior one.

Cervical vertebrae III and IV: There are no intercentra associated with the third and fourth cervical vertebrae. These elements display slender, vertically oriented neural spines, approximately twice as tall as they are long (Fig. 18). Similarly, tall neural spines are present in the anterior postaxial cervicals of *Proterosuchus* (NMQR 1484) and *Garjainia* (PIN 2394/5-10), as well as in most archosauriforms (Ezcurra, 2016; Ezcurra et al., 2019). On the other hand, the anterior postaxial cervicals of tanystropheids, *Azendohsaurus* (FMNH PR 2791) and *Prolacerta* (e.g. BP/1/2675) display low, anteroposteriorly elongated neural spines. Although the anterior margins of the neural spines are straight, the posterior margin bears a well-developed projection close to the mid-point between the dorsal margin of the neural spine and the beginning of the postzygapophysis in cervical vertebra III. The neural spine of the fourth cervical is dorsally broken and scattered, but a similar projection seems to be present. The dorsal surface of the neural spine lacks a transverse expansion in the third cervical, but in the fourth element this condition is unclear. This condition contrasts with *Prolacerta* (e.g. BP/1/2675) and proterosuchids (e.g. *Proterosuchus*, NMQR 1484), which have neural spines gradually expanding towards their distal ends. The prezygapophyses are anteroposteriorly long and transversely wide, with mainly horizontal articulation surfaces. The postzygapopophysis of cervical vertebra III is approximately at the same level as the prezygapophysis, whereas in cervical IV the postzygapophysis is placed considerably dorsally to the prezygapophysis. What seems to be a weak interzygapophyseal lamina is present in cervical III. A similar lamina is present on the

third cervical vertebra of *Prolacerta* (BP/1/2675). Although the bone surface in this region is poorly preserved both in cervical III and IV, shallow depressions are present at the bases of the neural spines of these elements. Excavations at the base of the neural spine are present in the anterior cervicals of *Prolacerta*, *Proterosuchus*, erythrosuchids and other crownward archosauriforms (Ezcurra, 2016, character 337).

The centra are slightly anteroposteriorly expanded, and their anterior and posterior articulation surfaces are positioned approximately at the same level (the posterior articulation surface is slightly ventrally displaced in cervical IV). The diapophyses and parapophyses are located approximately at the dorsoventral midpoints of the centra in both cervicals III and IV. A longitudinal lamina extending posteriorly from the diapophysis is present in both elements, although this structure seems to be better developed in cervical IV, in which it dorsally limits a deep depression on the centrum. Similar laminae are present in *Proterosuchus* (NMQR 1484), and are widely expanded in some other early archosauriform taxa (e.g. *Chasmatosuchus,* PIN 2252/381). Delicate, horizontally-directed, cervical ribs are associated with cervicals III and IV. No neurocentral suture is distinguishable.

PHYLOGENETIC ANALYSES

Our first analysis (updated scores of *Teyujagua paradoxa* in the data matrix of Pinheiro et al. 2016) resulted in eight most parsimonious trees (MPTs) of 879 steps (differing from two MPTs of 872 steps in the original analysis), with CI = 0.34, RI = 0.62. The strict consensus of these trees (Fig. 19) displays the same relationships recovered by Pinheiro et al. (2016) for non-archosauriform archosauromorphs: Tanystropheidae (*Tanystropheus* + *Macrocnemus*) is recovered in a clade together with (*Protorosaurus* +

Aenigmastropheus); Rhynchosauria is recovered as monophyletic, but the relationships between the three included representatives of this clade are unresolved; *Prolacerta* is recovered as the sister-taxon to (*Teyujagua* + Archosauriformes); and *Teyujagua* is consistently placed as the sister-taxon to Archosauriformes (Bremer support 3 for this node). Relationships among Archosauriformes are, however, mainly unresolved, with a major polytomy including proterosuchid taxa, *Chanaresuchus*, *Koilamasuchus*, *Fugusuchus*, (*Vancleavea* + *Doswellia*), Euparkeridae, Erythrosuchidae and Archosauria (which is recovered as monophyletic).

Synapomorphies of the clade (*Teyujagua* + Archosauriformes) in the consensus tree of analysis I include: serrations on marginal tooth crowns (character 4); trapezoidal infratemporal fenestrae (character 17); presence of a palatal process on the premaxillae (character 25); absence of an anterior maxillary foramen (character 29); absence of a posterolateral process on the frontal (character 42); reduced postfrontals (character 43); presence of an external mandibular fenestra (character 105); and presence of a lateral shelf on the surangular (character 110).

Archosauriformes, on the other hand, is supported by three unambiguous synapomorphies: presence of antorbital fenestrae (character 12); complete lower temporal bar (character 19); and posteroventral process of premaxilla extending posterior to the external naris (character 252)

Analysis II (updated scores of *T. paradoxa* in the dataset of Butler et al., 2019, which is, by its turn, derived from the original data matrix of Ezcurra, 2016) resulted in 44 trees of 3599 steps in the first round of searches using the New Technology option of TNT (FUSE algorithm, 100 hits). A second round of TBR starting from the trees recovered in the first round, found 54 trees of 3599 steps, CI = 0.25; RI = 0.65. The strict consensus of the most parsimonious trees produced by analysis II shows that

Teyujagua is consistently nested as the sister group of a clade formed by *Tasmaniosaurus triassicus* and Archosauriformes (Fig. 20). The clade (*Teyujagua* + (*Tasmaniosaurus triassicus* + Archosauriformes)) is supported by the absence of an anterior maxillary foramen (character 52); presence of a distinct ascending process with a posterior concave margin on the maxilla (character 58); upper temporal bar level with the dorsal margin of the orbit (character 126); gentle transition between the anterior and ventral processes of squamosal (character 139); squamosal contributes with more than a half of the posterior border of the infratemporal fenestra (character 146); presence of an external mandibular fenestra (character 262); serrated teeth (character 304) and excavation at the base of postaxial neural spines (character 337).

Notably, given the node-based definition of Archosauriformes (Nesbitt, 2011; Ezcurra, 2016), the inclusion of *Tasmaniosaurus triassicus* in the dataset of Butler et al. (2019) makes this enigmatic archosauromorph the sister-taxon to Archosauriformes (*contra* Pinheiro et al., 2016), even though it closely resembles proterosuchid archosauriforms in several aspects (Ezcurra, 2014). Synapomorphies supporting (*Tasmaniosaurus* + Archosauriformes) are: presence of antorbital fenestrae (character 13); sheet-like postparietal (character 171) and presence of a posterocentral process on the dentary (character 273).

In addition, the strict consensus recovered by analysis II agrees with previous assessments of archosauromorph phylogeny (e.g. Ezcurra, 2016; Sengupta et al., 2017; Butler et al., 2019). *Jesairosaurus lehmani* is the sister taxon to a monophyletic Tanystropheidae, and the clades Allokotosauria, Rhynchosauria, Erythrosuchidae, Proterochampsia and Archosauria were recovered. Notably, there is a polytomy including *Boreopricea*, (*Kadimakara* + *Prolacerta*) and (*Teyujagua* + (*Tasmaniosaurus* + Archosauriformes)).

DISCUSSION

IMPLICATIONS FOR THE EARLY EVOLUTION OF ARCHOSAURIFORMES

Shaping the archosauriform skull. The archosauriform body plan was classically characterized by a series of key cranial characters presumably related to hypercarnivory (Gauthier, 1986; Nesbitt; 2011; Ezcurra et al. 2014). Even though the clade and its characteristic morphology had already evolved by the latest Permian (Ezcurra et al., 2014), adaptations to carnivory provided archosauriforms with the opportunity to replace large synapsids as apex predators during the aftermath of the end-Permian mass extinction (Ezcurra & Butler, 2018). As such, in the Karoo Basin of South Africa, where Permian-Triassic sequences are well-preserved and extensively studied, the archosauriform *Proterosuchus* is the first new taxon to appear in the lowermost Triassic rocks following the extinction (Botha & Smith, 2006).

Since the discovery of *Teyujagua paradoxa*, however, it has become clear that some characteristic features of Archosauriformes evolved in a mosaic fashion before the emergence of this clade (Pinheiro et al., 2016). Similar to non-archosauriform archosauromorphs, *Teyujagua* lacks antorbital fenestrae and still retains open lower temporal bars. However, *Teyujagua* also displays cranial features that were previously regarded as synapomorphic for Archosauriformes, such as serrated teeth and external mandibular openings. The inclusion of *Teyujagua* in a broader phylogenetic dataset of Archosauromorpha makes it possible to track the origins of these key features.

As discussed above, although the overall morphology of *Tasmaniosaurus triassicus* closely resembles those of proterosuchids (Ezcurra, 2014), the node-based phylogenetic definition of Archosauriformes proposed by Nesbitt (2011) excludes this

species from the clade. This means that *Teyujagua* is the sister taxon of (*Tasmaniosaurus* + Archosauriformes), and not the sister taxon to Archosauriformes, as previously proposed by Pinheiro et al. (2016). The distribution of character states among archosauriforms and closely related taxa reveals that classic synapomorphies of Archosauriformes, most of them regarding skull morphology, in fact appear earlier among its successive sister taxa (e.g. *Teyujagua*, *Tasmaniosaurus*). Serrated teeth, external mandibular fenestrae and an elevated upper temporal bar (related to the enlargement of the adductor chamber) characterize the clade formed by *Teyujagua*, *Tasmaniosaurus* and Archosauriformes. Remarkably, all those features are linked to the development of carnivory, making archosauriforms and its close sister taxa pre-adapted to fill the role of apex predators already during the Permian, when they were minor components of terrestrial faunas.

In addition to dietary adaptations, the clade composed of *Tasmaniosaurus* and archosauriforms further developed facial pneumaticity, which was already incipient in *Teyujagua* and *Prolacerta* (see below), also evolving some secondary skull features, such as a sheet-like postparietal and posterocentral processes on the dentaries. Finally, in this new phylogenetic framework, only two synapomorphies support Archosauriformes: the presence of interdental plates and dorsally curved dentaries. This is probably a result of the fragmentary nature of *Tasmaniosaurus* holotype, as the ubiquitous presence of missing data in the taxon makes ambiguous several Archosauriformes potential synapomorphies.

The origin of the antorbital fenestrae. The antorbital fenestra has been consistently found as a synapomorphy of Archosauriformes or a node more basal (e.g. Gauthier et al., 1988; Nesbitt, 2011; Pinheiro et al., 2016; Ezcurra, 2016), being classically

considered as the main diagnostic feature of this clade (Witmer, 1997). The antorbital fenestrae are openings in the skull positioned anterior to the orbits, which are often large in size, and which are mostly delimited by the maxillae and lacrimals, although sometimes with contributions from the nasals and/or jugals (Witmer, 1997). The internal antorbital fenestrae (*sensu* Witmer, 1997) are usually surrounded by the antorbital fossae, which are normally most extensively developed on the maxillae, but which can also excavate other adjacent bones. The development of additional openings within the antorbital fossa is also common in archosauriforms – for example, the promaxillary foramen of many theropod dinosaurs (Witmer, 1997).

The function of the antorbital fenestrae, fossae and accessory openings remained elusive until detailed anatomical study by Witmer (1987, 1995a, 1997), which applied the extant phylogenetic bracket approach (Witmer, 1995b) to convincingly argue that these structures housed paranasal air sinuses, epithelial air sacs that outgrow the cartilaginous nasal capsule, partially filling the nasal cavity and pneumatizing facial bones. Although they fall outside the phylogenetic bracket formed by extant birds and crocodilians (both of which display prominent paranasal sinuses), early archosauriforms such as *Proterosuchus* and *Euparkeria* already display all the osteological correlates for these soft tissue structures, and the evidence for intense pneumatization in early archosauriform skulls is compelling.

Proterosuchus, the earliest archosauriform for which the cranial anatomy is well understood, displays large antorbital fenestrae bounded by the maxillae and lacrimals, with a small contribution to the posteroventral corners of the fenestrae from the maxillary rami of the jugals. Shallow lacrimal antorbital fossae are present, indicating that paranasal air sacs partially covered the lateral surfaces of these bones, but antorbital fossae are absent from the lateral surface of maxillae (Ezcurra, 2016). Wider and

deeper antorbital fossae excavating the maxillae laterally in addition to the lacrimals appear for the first time among erythrosuchids such as *Erythrosuchus* and *Garjainia* (Gower, 2003; Ezcurra, 2016; Ezcurra et al., 2019), where they occur primarily upon the ascending processes of the maxillae, and in early crown archosaurs the antorbital fossae are most extensive, extending onto the horizontal process of the maxilla along the entire ventral margins of the antorbital fenestrae.

Although it lacks antorbital fossae or fenestrae on the external surface of the skull, given its phylogenetic position the morphologies of the facial bones of *Teyujagua* may shed light on the initial development of these key anatomical features. As described above, the medial surfaces of the maxillae of *Teyujagua* bear deep, arrowhead-shaped depressions, lateral to which the maxillary wall is exceptionally thin (Fig. 21A, C). These depressions, which we here refer to as medial antorbital fossae, are contiguous with similar excavations on the nasals and lacrimals. Together, they probably formed a single functional structure. *Prolacerta*, which was generally considered as the sister-taxon to Archosauriformes prior to the description of *Teyujagua*, possesses very similar arrow-shaped medial antorbital fossae on the maxillae (BP/1/2675) (Fig. 21B).

Topological similarities and phylogenetic congruence lead us to hypothesize homology between the medial antorbital fossae of *Teyujagua* and *Prolacerta* and the antorbital fenestrae and associated fossae of archosauriforms. In this framework, skull pneumaticity associated with the lateral expansion of epithelial air sacs from the nasal capsule appeared internally on the medial surfaces of the facial bones, before it became expressed laterally via the antorbital fenestrae. Thus, integrating new data from *Teyujagua* and *Prolacerta* with existing knowledge of the morphological diversity of facial bones among Archosauriformes, we recognize five, not necessarily

interdependent, steps in the evolution of archosauriform antorbital fenestration (Fig. 22):

I) *Lateral outgrowth of epithelial sinuses from the cartilaginous nasal capsule*. Air sacs are restricted to the nasal chamber, and not expressed on the lateral surfaces of the skull. Osteological correlates are the presence of medial excavations on facial bones, forming the medial antorbital fossae described above. Of the two taxa known to show these fossae, *Teyujagua* differs from *Prolacerta* in having broader lacrimals that display medial excavations, possibly also as a consequence of skull pneumatization. In *Prolacerta*, therefore, the air sacs would be more restricted to the maxillary portion of the snout than in *Teyujagua*.

II) *Opening of the antorbital fenestrae*. Continued growth of lateral sinuses would drive facial bones to ossify surrounding the air sacs, resulting in the appearance of antorbital fenestrae on the lateral surfaces of the skull. This would be driven by the reduction in size of the lacrimals (broad in *Teyujagua*), and also by the development of a separation between the ascending and the horizontal or posterior processes of the maxillae. This condition could result from the formation of a fontanelle between the lacrimals and maxillae that would remain open in later ontogenetic stages, as was observed by Witmer (1995) for extant birds. At this stage only the lacrimals display shallow fossae, as observed for example in some specimens of *Proterosuchus* (e.g. RC 846).

III) *Lateral excavation of bones surrounding the antorbital fenestrae*. The paranasal sinuses invade the lateral surface of the skull, resulting in deep excavations with well-defined rims on some facial bones. These excavations, the antorbital fossae, are usually located on the lacrimals and maxillae, but can sometimes extend onto the nasals and/or jugals. Deep antorbital fossae with well-defined rims are characteristic of

the clade formed by erythrosuchids and Eucrocopoda (euparkeriids, Proterochampsia and archosaurs), and expand further such that they extend along the entire horizontal process of the maxilla in crown archosaurs (Nesbitt, 2011; Ezcurra, 2016).

IV) *Emergence of accessory cavities.* The development of secondary epithelial diverticula associated with the main corpus of the paranasal sinus creates a series of recesses in the bones that surround the antorbital fenestrae (Witmer, 1997). These accessory openings are reasonably common among dinosaurs (especially theropods), but also occur in pterosaurs, some loricatans (Witmer, 1997) and in at least one basal sauropodomorph (*Macrocollum itaquii*, CAPPA/UFSM 0001a; Müller et al., 2018).

V) *Reduction of the antorbital complex/closure of the antorbital fenestrae.* Several clades experienced the reductions of the antorbital fossae and fenestrae and eventual closure of the latter as the result of different selective pressures and biomechanical contingencies (Witmer, 1997). A number of representatives of the non-archosaurian archosauriform clade Proterochampsia display reduced, dorsally-positioned antorbital fenestrae with poorly developed antorbital fossae (e.g. Trotteyn et al., 2013). This trend may be a result of the susceptibility of dorsoventrally compressed skulls to torsion loads, as was proposed by Witmer (1997) for crocodylomorphs. The apparently fully aquatic proterochampsian *Vancleavea* reached the extreme of completely lacking external antorbital openings (Nesbitt et al., 2009), a condition later independently acquired by neosuchian crocodylomorphs. Among Neosuchia, the reduction and latter closure of the antorbital cavities was probably linked to the formation of a secondary palate, as well as platyrostry (Witmer, 1997). Ornithischian dinosaurs also display a strong trend towards reduction and eventual loss of the antorbital openings, probably as a consequence of the development of specialized feeding apparatus (Witmer, 1997). In addition, the lack of antorbital fossae is the usual

condition for pterosaurs, with the exception of some few early representatives (Nesbitt & Hone, 2010), and the confluence of the nasal and antorbital fenestrae is characteristic of Pterodactyloidea (Kellner, 2003; Unwin, 2003).

On the presence of external mandibular fenestrae in non-archosauriform archosauromorphs. The recent recognition of external mandibular openings in *Teyujagua paradoxa* (Pinheiro *et al*. 2016) made this taxon the only non-archosauriform archosauromorph in which this classic archosauriform feature is unequivocally present (the condition in *Tasmaniosaurus* is dubious). The recovered phylogenetic relationships of *Teyujagua* implies that the presence of external mandibular fenestrae is a synapomorphy of *Teyujagua* + (*Tasmaniosaurus* + Archosauriformes).

The tanystropheid *Macrocnemus fuyuanensis*, however, was proposed as possibly possessing external mandibular openings. The brief description of the holotype by Li *et al.* (2007) only mentioned the presence of "mandibular fossae", not implying the presence of actual openings. However, in a subsequent description of a better-preserved specimen (Jiang et al., 2011), a small slit-like opening between the angular and the surangular was mentioned and illustrated, although the potential implications of the presence of external mandibular fenestrae in a tanystropheid were not discussed.

Our examination of several specimens of *Macrocnemus*, however, revealed that the posterior mandibular bones are often disarticulated and were probably only loosely connected in life. Indeed, some European specimens of *Macrocnemus*, such as PIMUZ T 1559 (attributed to *M*. aff. *M. fuyuanensis* by Jaquier et al., 2017), show that a similar opening to that illustrated by Jiang et al. (2011) can be artificially created by the combined effects of slightly displaced posterior mandibular elements and fragmentation

of some bones (Fig. 23). In PIMUZ T 1559, the surangular is anteriorly and ventrally abraded, and most of the angular and part of the splenial seem to be displaced from their original positions, creating an artificial lateral opening in the lower jaw. In addition, the presumed mandibular fenestra of *M. fuyuanensis* is biased by the misinterpretation by Jiang et al. (2010) of the splenial as a posteroventral ramus of a bifurcated dentary (Torsten Scheyer, personal communication, 2018). We note that posteriorly bifurcated dentaries are the typical condition for archosauriforms, but that among non-archosauriform archosauromorphs, only basal rhynchosaurs and *Tasmaniosaurus* show this feature (Ezcurra, 2014). The revaluation of *M. fuyuanensis* by Jaquier et al. (2017) did not identify external mandibular fenestrae in any of the specimens attributed to this taxon. As such, we consider it most likely that external mandibular fenestrae were not present in *M. fuyuanensis*.

CONCLUSIONS

Teyujagua paradoxa, as represented by its holotype and thus far only known specimen, has a unique morphology that distinguishes it from all other known archosauromorphs. In addition, *T. paradoxa* reveals the emergence of anatomical features that culminated in the assemblage of the typical archosauriform skull architecture, including the early development of cranial pneumaticity associated with the paranasal air sinuses. CT-based anatomical description of *T. paradoxa* provided a wealth of new information, allowing a reassessment of its phylogenetic relationships. The cladistic analysis performed here supported *T. paradoxa* as the sister taxon of (*Tasmaniosaurus* + Archosauriformes), in a similar position to that recovered by Pinheiro et al. (2016). In addition to adding information on character evolution during the origins of Archosauriformes, *T. paradoxa* plays an important role in the understanding of terrestrial ecosystems in the aftermath of the end-Permian mass extinction in western Gondwana.

REFERENCES

Barberena MC. 1981. Uma nova espécie de *Proterochampsa* (*P. nodosa*, sp. nov.) do Triássico do Brasil. *Anais da Academia Brasileira de Ciências* **54**: 127–141.

Benton MJ. 1983. The Triassic reptile *Hyperodapedon* from Elgin: Functional morphology and relationships. *Philosophical Transactions of the Royal Society of London. Series B, Biological Sciences* **302**: 605–718.

Benton MJ, Allen JL. 1997. *Boreopricea* from the Lower Triassic of Russia, and the relationships of the prolacertiform reptiles. *Palaeontology* **40**: 931–953.

Benton MJ, Tverdokhlebov VP, Surkov MV. 2004. Ecosystem remodeling among vertebrates at the Permian-Triassic boundary in Russia. *Nature* **432**: 97–100.

Botha J, Smith RMH. 2006. Rapid vertebrate recuperation in the Karoo Basin of South Africa following the End-Permian extinction. *Journal of African Earth Sciences* **45**: 502–514.

Brusatte SL, Benton MJ, Ruta M, Lloyd GT. 2008. Superiority, competition, and opportunism in the evolutionary radiation of dinosaurs. *Science* **321**: 1485–1488.

Butler RJ, Ezcurra MD, Liu J, Sookias RB, Sullivan C. 2019. The anatomy and phylogenetic position of the erythrosuchid archosauriform *Guchengosuchus shiguaiensis* from the earliest Middle Triassic of China. *PeerJ* **7**: e6435.

Butler RJ, Ezcurra MD, Montefeltro FC, Samathi A, Sobral G. 2015. A new species of basal rhynchosaur (Diapsida: Archosauromorpha) from the early Middle Triassic of South Africa, and the early evolution of Rhynchosauria. *Zoological Journal of the Linnean Society* **174**: 571–588.

Camp CL. 1945. *Prolacerta* and the protorosaurian reptiles. *American Journal of Science* **243**: 17–32.

Claessens LPAM, O'Connor P M, Unwin DM. 2009. Respiratory evolution facilitated the origin of pterosaur flight and aerial gigantism. *PLoS ONE* **4**: e4497.

Colbert EH. 1947. Studies of the phytosaurs *Machaeroprosopus* and *Rutiodon. Bulletin of the American Museum of Natural History* **88**: 55–96.

Da-Rosa AAS, Piñeiro G, Dias-da-Silva S, Cisneros JC, Feltrin FF, Neto LW. 2009. Bica São Tomé, um novo sítio fossilífero para o Triássico Inferior do sul do Brasil. *Revista Brasileira de Paleontologia* **12**: 67–76.

Dias-da-Silva S, Modesto SP, Schultz CL. 2006. New material of *Procolophon* (Parareptilia: Procolophonoidea) from the Lower Triassic of Brazil, with remarks on the ages of the Sanga do Cabral and Buena Vista Formations of South America. *Canadian Journal of Earth Sciences* **43**: 1685–1693.

Dias-da-Silva S, Pinheiro FL, Da-Rosa AAS, Martinelli AG, Schultz CL, Silva-Neves E, Modesto SP. 2017. Biostratigraphic reappraisal of the Lower Triassic Sanga do Cabral Supersequence from South America, with a description of new material attributable to the parareptile genus *Procolophon*. *Journal of South American Earth Sciences* **79**: 281–296.

Dilkes DW. 1995. The rhynchosaur *Howesia browni* from the Lower Triassic of South Africa. *Palaeontology* **38**: 665–685.

Dilkes DW. 1998. The Early Triassic rhynchosaur *Mesosuchus browni* and the interrelationships of basal archosauromorph reptiles. *Philosophical Transactions of the Royal Society B: Biological Sciences* **353**: 501–541.

Dilkes DW, Arcucci AB. 2012. *Proterochampsa barrionuevoi* (Archosauriformes: Proterochampsia) from the Late Triassic (Carnian) of Argentina and a phylogenetic analysis of Proterochampsia. *Palaeontology* **55**: 853–885.

Eltink E, Da-Rosa AAS, Dias-da-Silva S. 2017. A capitosauroid from the Lower Triassic of South America (Sanga do Cabral Supersequence: Paraná Basin), its phylogenetic relationships and biostratigraphic implications. *Historical Biology* **29**: 863–874.

Ewer RF. 1965. The anatomy of the thecodont reptile *Euparkeria capensis* Broom. *Philosophical Transactions of the Royal Society of London Series B, Biological Sciences* **751**: 379–435.

Ezcurra MD. 2014. The osteology of the basal archosauromorph *Tasmaniosaurus triassicus* from the Lower Triassic of Tasmania, Australia. *PLoS ONE* **9**: e86864.

Ezcurra MD. 2016. The phylogenetic relationships of basal archosauromorphs, with an emphasis on the systematics of proterosuchian archosauriforms. *PeerJ* **4**: e1778.

Ezcurra MD. 2017. Can social and sexual selection explain the bizarre snout of proterosuchid archosauriforms? *Historical Biology* **29**: 348–358.

Ezcurra MD, Butler RJ. 2015. Taxonomy of the proterosuchid archosauriforms (Diapsida: Archosauromorpha) from the earliest Triassic of South Africa, and implications for the early archosauriform radiation. *Palaeontology* **58**: 141–170.

Ezcurra MD, Butler RJ. 2018. The rise of the ruling reptiles and ecosystem recovery from the Permian-Triassic mass extinction. *Proceedings of the Royal Society B: Biological Sciences* **285**: 20180361.

Ezcurra MD, Gower DJ, Sennikov AG, Butler RJ. 2019. The osteology of the holotype of the early erythrosuchids *Garjainia prima* (Diapsida: Archosauromorpha) from the upper Lower Triassic of European Russia. *Zoological Journal of the Linnean Society* **185**: 717–783.

Ezcurra MD, Montefeltro F, Butler RJ. 2016. The early evolution of rhynchosaurs. *Frontiers in Ecology and Evolution* **3**: 142.

Ezcurra MD, Scheyer, TM, Butler RJ. 2014. The origin and early evolution of Sauria: Reassessing the Permian saurian fossil record and the timing of the crocodile-lizard divergence. *PLoS ONE* **9**: e89165.

Flynn JJ, Nesbitt SJ, Parrish JM, Ranivoharimanana L, Wyss AR. 2010. A new species of *Azendohsaurus* (Diapsida: Archosauromorpha) from the Triassic Isalo Group of southwestern Madagascar: cranium and mandible. *Palaeontology* **53**: 669–688.

França MA, Langer MC, Ferigolo J. 2013. The skull anatomy of *Decuriasuchus quartacolonia* (Pseudosuchia: Suchia: Loricata) from the Middle Triassic of Brazil. In: Nesbitt SJ, Desojo JB, Irmis RB, eds. *Anatomy, phylogeny and palaeobiology of early archosaurs and their kin*. London: Geological Society, Special Publication **379**, 469–501.

Gauthier J. 1986. Saurischian monophyly and the origin of birds. *Memoirs of the California Academy of Sciences* **8**: 1–55.

Gauthier J, Kluge AG, Rowe T. 1988. Amniote phylogeny and the importance of fossils. *Cladistics* **4**: 105–209.

Goloboff PA, Catalano SA. 2016. TNT version 1.5, including a full implementation of phylogenetic morphometrics. *Cladistics* **32**: 221–238.

Gottmann-Quesada A, Sander PM. 2009. A redescription of the early archosauromorph *Protorosaurus spenseri* Meyer, 1832 and its phylogenetic relationships. *Palaeontographica Abteilung A* **287**: 123–220.

Gower DJ. 2003. Osteology of the early archosaurian reptile *Erythrosuchus africanus* Broom. *Annals of the South African Museum* **110**: 1–84.

Jaquier VP, Fraser NC, Furrer H, Scheyer TM. 2017. Osteology of a new specimen of *Macrocnemus* aff. *M. fuyuanensis* (Archosauromorpha, Protorosauria) from the Middle Triassic of Europe: Potential implications for species recognition and paleogeography of tanystropheid protorosaurs. *Frontiers in Earth Science* **5**: 91.

Jetz W, Thomas GH, Joy JB, Hartmann K, Mooers AO. 2012. The global diversity of birds in space and time. *Nature* **491**: 444–448.

Jiang D, Rieppel O, Fraser NC, Motani R, Hao W, Tintori A, Sun Y, Sun Z. 2011. New information on the protorosaurian reptile *Macrocnemus fuyuanensis* Li et al., 2007, from the Middle/Upper Triassic of Yunnan, China. *Journal of Vertebrate Paleontology* **31**: 1230–1237.

Kellner AWA. 2003. Pterosaur phylogeny and comments on the evolutionary history of the group. In: Buffetaut E, Mazin J-M, eds. *Evolution and Palaeobiology of Pterosaurs* London: Geological Society, Special Publications **217**: 105–137.

Lacerda MB, Mastrantonio BM, Fortier DC, Schultz CL. 2016. New insights on *Prestosuchus chiniquensis* Huene, 1942 (Pseudosuchia, Loricata) based on new specimens from the “Tree Sanga” Outcrop, Chiniquá Region, Rio Grande do Sul, Brazil. *PeerJ* **4**: e1622.

Langer MC, Schultz CL. 2003. A new species of the Late Triassic rhynchosaur *Hyperodapedon* from the Santa Maria Formation of South Brazil. *Palaeontology* **43**: 633–652.

Li C, Zhao L, Wang L. 2007. A new species of *Macrocnemus* (Reptilia: Protorosauria) from the Middle Triassic of southwestern China and its palaeogeographical implication. *Science in China Series D: Earth Sciences* **50**: 1601–1605.

Maddison WP, Maddison DR. 2018. Mesquite: a modular system for evolutionary analysis. Version 3.51 http://www.mesquiteproject.org.

Mastrantonio BM, von Baczo MB, Desojo JB, Schultz, CL. 2019. The skull anatomy and cranial endocast of the pseudosuchid archosaur *Prestosuchus chiniquensis* from the Triassic of Brazil. *Acta Palaeontologica Polonica* **64**.

Modesto SP, Sues H-D. 2004. The skull of the Early Triassic archosauromorph reptile *Prolacerta broomi* and its phylogenetic significance. *Zoological Journal of the Linnean Society* **140**: 335–351.

Montefeltro FC, Langer MC, Schultz CL. 2010. Cranial anatomy of a new genus of hyperodapedontine rhynchosaur (Diapsida: Archosauromorpha) from the Upper Triassic of southern Brazil. *Earth and Environmental Science Transactions of the Royal Society of Edinburgh* **101**: 27–52.

Müller RT, Langer MC, Dias-da-Silva S., 2018. An exceptionally preserved association of complete dinosaur skeletons reveals the oldest long-necked sauropodomorphs. *Biology Letters* **14**: 20180633.

Nesbitt SJ. 2011. The early evolution of archosaurs: relationships and the origin of major clades. *Bulletin of the American Museum of Natural History* **352**: 1–292.

Nesbitt SJ, Stocker MR, Small BJ, Downs A. 2009. The osteology and relationships of *Vancleavea campi* (Reptilia: Archosauriformes). *Zoological Journal of the Linnean Society* **157**: 814–864.

Nesbitt SJ, Flynn JJ, Pritchard AC, Parrish JM, Ranivoharimanana L, Wyss AR. 2015. Postcranial anatomy and relationships of *Azendohsaurus madagaskarensis*. *Bulletin of the American Museum of Natural History* **398**: 1–126.

Nosotti S. 2007. *Tanystropheus longobardicus* (Reptilia, Protorosauria): re-interpretations of the anatomy based on new specimens from the Middle Triassic of Besano (Lombardy, Northern Italy). *Memorie della Societa Italiana di Scienze Naturali e del Museo Civico di Storia Naturale di Milano* **35**: 1–88.

Oliveira TMO, Oliveira D, Schultz CL, Kerber L, Pinheiro FL. 2018. Tanystropheid archosauromorphs in the Lower Triassic of Gondwana. *Acta Palaeontologica Polonica* **63**.

Ösi A, Prondvai E, Frey E, Pohl B. 2010. New interpretation of the palate of pterosaurs. *The Anatomical Record* **293**: 243–258.

Pinheiro FL, França MA, Lacerda MB, Butler RJ, Schultz CL. 2016. An exceptional fossil skull from South America and the origins of the archosauriform radiation. *Scientific Reports* **6**: 22817.

Roberto-da-Silva L, França MAG, Cabreira SF, Müller RT, Dias-da-Silva. 2016. On the presence of the subnarial foramen in *Prestosuchus chiniquensis* (Pseudosuchia: Loricata) with remarks on its phylogenetic distribution. *Anais da Academia Brasileira de Ciências* **88**: 1309–1323.

Roberto-da-Silva L, Müller RT, França MAG, Cabreira SF, Dias-da-Silva S. 2018. An impresive skeleton of the giant top predator *Prestosuchus chiniquensis* (Pseudosuchia: Loricata) from the Triassic of Southern Brazil, with phylogenetic remarks. *Historical Biology*.

Schultz CL, Langer MC, Montefeltro FC. 2016. A new rhynchosaur from south Brazil (Santa Maria Formation) and rhynchosaur diversity patterns across the Middle-Late Triassic boundary. *Paläontologische Zeitschrift* **90**: 593–609.

Sen K. 2003. *Pamelaria dolichotrachela*, a new prolacertids reptile from the Middle Triassic of India. *Journal of Asian Earth Sciences* **21**: 663–681.

Sengupta S, Ezcurra MD, Bandyopadhyay S. 2017. A new horned and long-necked herbivorous stem-archosaur from the Middle Triassic of India. *Scientific Reports* **7**: 8366.

Sereno PC, Novas FE. 1993. The skull and neck of the basal theropod *Herrerasaurus ischigualastensis*. *Journal of Vertebrate Paleontology* **13**: 451–476.

Silva-Neves E, Modesto SP, Dias-da-Silva. 2018. A new, nearly complete skull of *Procolophon trigoniceps* Owen, 1876 from the Sanga do Cabral Supersequence, Lower Triassicof Southern Brazil, with phylogenetic remarks. *Historical Biology*.

Spiekman SN. 2018. A new specimen of *Prolacerta broomi* from the lower Fremouw Formation (Early Triassic) of Antarctica, its biogeographical implications and a taxonomic revision. *Scientific Reports* **8**: 17996.

Trotteyn MJ, Arcucci AB, Raugust T. 2013. Proterochampsia: an endemic archosauriform clade from South America. In: Nesbitt SJ, Desojo JB, Irmis RB, eds.

Anatomy, phylogeny and palaeobiology of early archosaurs and their kin. London: Geological Society, Special Publication **379**, 59–90.

Unwin DM. 2003. On the phylogeny and evolutionary history of pterosaurs. In: Buffetaut E, Mazin J-M, eds. *Evolution and Palaeobiology of Pterosaurs.* London: Geological Society, Special Publications **217**: 139–190.

Welman J. 1998. The taxonomy of the South African proterosuchids (Reptilia, Archosauromorpha). *Journal of Vertebrate Paleontology* **18**: 340–347.

Witmer LM. 1987. The nature of the antorbital fossa of archosaurs: Shifting the null hypothesis. In: Currie PJ, Koster EH, eds. *Fourth Symposium on Mesozoic Terrestrial Ecosystems, Short Papers*. Drumheller: Royal Tyrrell Museum of Palaeontology: 230–235.

Witmer LM. 1995a. Homology of facial structures in extant archosaurs (birds and crocodilians), with special reference to paranasal pneumaticity and nasal conchae. *Journal of Morphology* **225**: 269–327.

Witmer LM. 1995b. The extant phylogenetic bracket and the importance of reconstructing soft tissues in fossils. In: Thomason JJ, ed. *Functional Morphology in Vertebrate Paleontology*. New York: Cambridge University Press: 19–33.

Witmer LM. 1997. The evolution of the antorbital cavity of archosaurs: A study in soft-tissue reconstruction in the fossil record with an analysis of the function of pneumaticity. *Journal of Vertebrate Paleontology* **17(Supplement)**: 1–73.

Zerfass H, Lavina EL, Schultz CL, Garcia AJV, Faccini UF, Chemale F. 2003. Sequence stratigraphy of continental Triassic strata of southermost Brazil: a

contribution to southwestern Gondwana paleogeography and paleoclimate. *Sedimentary Geology* **161**: 85–105.

APPENDIX

Updated scorings of *Teyujagua paradoxa* in the dataset of Pinheiro et al. (2016):

101110000? 20--121131 1000111000 1021001110 0010000001 100010-000 --
11201??? ?100????0? 2????????? ?????????? ?001100011 ?121??1?20 0??1??????
?????????? ?????????? ?????????? ?????????? ?????????? ?????????? ??????????
?????????? ?????????? ?????????? ?????????? ?????????? 00

Updated scorings of *Teyujagua paradoxa* in the dataset of Butler et al. (2019):

0?00000010 110-011011 1011?01210 000-20000 1200100-1- ?00---1100 1--000-000
1000310000 -0-010-00 00100-0001 0000-00000 000000-0-? ?1000100-0 1000100010
0000010000 ------1100 -0-1110110 2-10012000 010???2000 ?10?012?1? ?2?????010
?0101????? ?????????? ?????????? ?????????? ?0???????? 011?00000? 010-0-0000
0021?10?10 01?00??110 10011000?1 ?01??????0 0--??0?001 0?10?01?10 0000?1??10
?????????? ?????????? ?????????? ?????????? ?????????? ?????????? ??????????
?????????? ?????????? ?????????? ?????????? ?????????? ?????????? ??????????
?????????? ?????????? ?????????? ?????????? ?????????? ?????????? ??????????
?????????? ?????????? ????????0-- --------?? ??????000- 000------- -00-000000 0-000-
0?0? 0?????00-0 1?0?0?00?? ?????????? ??????0000 ?????????0 010??

Figure captions

Figure 1. UNIPAMPA 653, holotype of *Teyujagua paradoxa*, skull in right lateral (A), left lateral (B) and dorsal (C) views.

Figure 2. UNIPAMPA 653, holotype of *Teyujagua paradoxa*, interpretative drawings of skull in right lateral (A), left lateral (B) and dorsal (C) views. Abbreviations: an, angular; ar, articular; ax, axis; cv, cervical vertebra; d, dentary; emf, external mandibular fenestra; f, frontal; j, jugal; la, lacrimal; m, maxilla; n, nasal; p, parietal; pm, premaxilla; po, postorbital; pof, postfrontal; pp, paroccipital process; prf, prefrontal; q, quadrate; sa, surangular; so, supraoccipital; sp, splenial; sq, squamosal; st, supratemporal. Artwork by Joana Bruno.

Figure 3. Premaxilla of holotype of *Teyujagua paradoxa* (UNIPAMPA 653). Right premaxilla in lateral (A), medial (B), ventral (C) and dorsal (D) views; anterior skull bones in dorsolateral view (E, F); rendering of the right premaxilla with teeth inserted

(G). Abbreviations: I-IV, premaxillary tooth positions I-IV; d, dentary; m, maxilla; n, nasal; nfo, nasal fossa; pdp, posterodorsal process of premaxilla; pm, premaxilla; ptp, palatal process of premaxilla.

Figure 4. Maxilla of holotype of *Teyujagua paradoxa* (UNIPAMPA 653). Right maxilla in lateral (A), medial (B), ventral (C) and dorsal (D) views; photograph (E) and interpretative diagram (F) of anterior skull bones in right lateral view. Abbreviations: afj, articulation facet with jugal; afn, articulation facet with nasal; afpm, articulation facet with premaxilla; an, angular; apm, ascending process of maxilla; d, dentary; j, jugal; la, lacrimal; m, maxilla; maf, medial antorbital fossa; pm, premaxilla; po, postorbital; ppm, posterior process of maxilla; prf, prefrontal; sa, surangular; sp, splenial.

Figure 5. Nasal of holotype of *Teyujagua paradoxa* (UNIPAMPA 653). Right nasal in dorsal (A), ventral (B), medial (C) and lateral (D) views. Abbreviations: afm, articulation facet with maxilla; afpf, articulation facet with prefrontal; apn, anterior process of nasal; lpn, lateral process of nasal. Arrows indicate anterior direction.

Figure 6. Lacrimal of holotype of *Teyujagua paradoxa* (UNIPAMPA 653). Right lacrimal in lateral (A), medial (B), dorsal (C), ventral (D), anterior (E) and posterior (F) views. Abbreviations: apl, anterior process of lacrimal; nld, nasolacrimal duct. Arrows indicate anterior direction.

Figure 7. Jugal, postorbital and postfrontal of holotype of *Teyujagua paradoxa* (UNIPAMPA 653). Right jugal in lateral (A), medial (B), anterior (C), posterior (D), dorsal (E) and ventral (F) views; jugal in articulation with postorbital and postfrontal in lateral (G) view. Abbreviations: apj, ascending process of jugal; j, jugal; mpj, maxillary

process of jugal; po, postorbital; pof, postfrontal; ppj, posterior process of jugal. Arrows indicate anterior direction.

Figure 8. Holotype of *Teyujagua paradoxa* (UNIPAMPA 653). Photograph (A) and interpretative diagram (B) of posterior skull bones in left lateral view. Abbreviations: an, angular; la, lacrimal; m, maxilla; nld, nasolacrimal duct; po, postorbital; prf, prefrontal; q, quadrate; sa, surangular; sp, splenial; sq, squamosal.

Figure 9. Holotype of *Teyujagua paradoxa* (UNIPAMPA 653). Frontals and parietals in dorsal view (A); photograph (B) and interpretative diagram (C) of posterior skull bones in dorsal view. Abbreviations: f, frontal; j, jugal; m, maxilla; p, parietal; pf, parietal foramen; pof, postfrontal; po, postorbital; prf, prefrontal; sq, squamosal; st, supratemporal; stf, supratemporal fenestra.

Figure 10. Holotype of *Teyujagua paradoxa* (UNIPAMPA 653). Dorsal view of the skull detailing circumorbital ornamentation (arrowheads).

Figure 11. Postorbital and postfrontal of holotype of *Teyujagua paradoxa* (UNIPAMPA 653). Right postorbital and postfrontal in right lateral (A), medial (B), dorsal (C), ventral (D), anterior (E) and posterior (F) views. Abbreviations: pofr, postfrontal; ppo, posterior process of postorbital; vppo, ventral process of postorbital. Arrows indicate anterior direction.

Figure 12. Squamosal of holotype of *Teyujagua paradoxa* (UNIPAMPA 653). Right squamosal in lateral (A), medial (B), dorsal (C), ventral (D), posterior (E) and anterior (F) views. Abbreviations: aps, anterior process of squamosal; mps, medial process of squamosal; vps, ventral process of squamosal.

Figure 13. Posterolateral photograph (A) and interpretative diagram (B) of the skull of holotype of *Teyujagua paradoxa* (UNIPAMPA 653), detailing the left quadrate and

squamosal. Abbreviations: ecte, ectepicondyle; q, quadrate; qf, quadrate foramen; sq, squamosal.

Figure 14. Posterodorsal photograph (A) and interpretative diagram (B) of holotype of *Teyujagua paradoxa* (UNIPAMPA 653) detailing occipital bones. Abbreviations: cv, cervical vertebrae; fm, foramen magnum; p, parietal; pp, paroccipital process; ptf, post-temporal fenestra; so, supraoccipital; st, supratemporal.

Figure 15. Lower jaw of holotype of *Teyujagua paradoxa* (UNIPAMPA 653). Right dentary and articulated splenial after rendering in lateral (A), dorsal (B) and medial (C) views; interpretative diagram (D) of lower jaw in right lateral view, with artificial insertion of dentary rendering Abbreviations: an, angular; ar, articular; d, dentary; sa, surangular; sp, splenial.

Figure 16. Marginal dentition of holotype of *Teyujagua paradoxa* (UNIPAMPA 653). Tomographic slice of marginal dentition in transverse section (A), arrows indicate bone striae ankylosing the teeth to surrounding alveoli; photograph of posterior maxillary teeth in lateral view (B), the arrow indicates serrations associated with the distal carina; marginal maxillary and premaxillary dentition in right lateral view (C).

Figure 17. Marginal and palatal dentition of holotype of *Teyujagua paradoxa* (UNIPAMPA 653). Dentition in palatal view (A); teeth associated with left pterygoid and palatine in palatal view (B); dentition in right lateral (C) and left lateral (D) views. Arrows indicate anterior end of the skull; dashed line indicates inferred pterygoid outline. Abbreviations: T2-T4, pterygoid tooth fields according to Welman (1998); md, maxillary dentition; pd, palatal dentition; pld, palatine dentition; vd, vomerine dentition.

Figure 18. Photograph (A) and digital rendering (B) of cervical vertebrae of holotype of *Teyujagua paradoxa* (UNIPAMPA 653) in left lateral view. Abbreviations: ain, axis

intercentrum; ana, atlas neural arch; at, atlas; ati, atlas intercentrum. ax, axis; cr, cervical rib; cv III, cervical vertebra III; cv IV, cervical vertebra IV; dp, diapophysis; ns, neural spine; poz, postzygapophysis.

Figure 19. Strict consensus tree recovered by heuristic analysis of the dataset of Pinheiro et al. (2016) including updated scores for *Teyujagua paradoxa*. Artwork by Márcio L. Castro.

Figure 20. Strict consensus tree recovered by heuristic analysis of the dataset of Butler et al. (2019) including updated scores for *Teyujagua paradoxa*. Artwork by Márcio L. Castro.

Figure 21. Maxilla of *Teyujagua paradoxa* (UNIPAMPA 654) (A) (mirrored) and *Prolacerta broomi* (BP/1/2675) (B) in medial view; µCT-based rendering of rostrum of UNIPAMPA 653 in right lateral view (C), depicting internal structure of the skull. Not to scale. Abbreviation: maf, medial antorbital fossa. Photograph of *Prolacerta* courtesy of Martín Ezcurra.

Figure 22. Simplified phylogenetic relationships of selected archosauromorphs, displaying key steps of antorbital fenestrae evolution within the clade. Artwork of skulls by Márcio L. Castro.

Figure 23. *Macrocnemus* aff. *fuyuanensis* (PIMUZ T 1559). Photograph (A) and interpretative diagram (B) of lower jaw in left lateral view. Abbreviations: an, angular; ar, articular; c, coronoid; d, dentary; pa, prearticular; sa, surangular; sp, splenial.

Figure 24. Dawn of the Triassic in southwestern Gondwana. Artistic representation of Sanga do Cabral Formation fauna, with the parareptile *Procolophon* in the foreground, *Teyujagua* in the midground and several individuals of the temnospondyl *Tomeia* in the background. Artwork copyright Mark Witton.

Table 1. Measurements of holotype UNIPAMPA 653

Skull	
Total length (from the rostral end of premaxilla to the ectocondyle of the left quadrate)	114.5 mm
Maximum height (from the ventral edge of the right jugal to the posterior limits of the posterolateral process of parietal)	35 mm
Maximum width (between the lateral borders of both jugals)	62.5 mm
Maximum diameter of the supratemporal opening (right side of skull)	21.2 mm
Maximum height of the infratemporal opening (left side of skull)	22.6 mm
Orbital length (right orbit)	21.25 mm
Orbital height (right orbit)	19.1 mm
Nasal opening maximum length	30.3 mm
Nasal opening maximum width	12.9 mm
Premaxilla	
Total length (from the anterior border of the alveolar margin to the posterior end of the posterodorsal process)	22 mm
Main body length	12.6 mm
Maximum height (from the ventral surface of the alveolar margin to the dorsal margin of the posterodorsal process)	11.5 mm
Maximum width (from the medial suture to the lateral margin of the main body)	6.5 mm
Maxilla	
Total length (from the contact with premaxilla to the posterior end of the jugal process)	56.7 mm
Maximum height (from the alveolar margin to the dorsal end of the ascending process)	17.3 mm
Nasal	
Maximum length (form the anterior tip of the lateral process to the presumed suture with frontal – right element)	29.3 mm
Maximum width	9.5 mm

Lacrimal	
Maximum exposed length (right element)	12.6 mm
Maximum exposed height (right element)	12 mm
Jugal	
Total length (left element)	40 mm
Maximum height (right element)	21.7 mm
Prefrontal	
Total length (right element)	19.8 mm
Maximum width	6.8 mm
Frontal	
Total length	21.9 mm
Maximum width (from the medial suture to the orbital margin)	10.3 mm
Parietal	
Maximum length (from suture with frontal to the posterior border of the posterolateral process – right element)	22 mm
Maximum width (from medial suture to the most lateral border)	13.5 mm
Minimum width between the supratemporal openings	9.8 mm
Postfrontal	
Maximum transverse width (right element)	12.1 mm
Posteromedial-anterolateral length (right element)	6.15 mm
Postorbital	
Height (from the ventral tip of the jugal process to the dorsal margin of the main body – right element)	20.1 mm
Anteroposterior length (main body – right element)	17.4 mm
Squamosal	
Exposed anteroposterior length (right element)	18.6 mm
Height (left element)	24 mm
Supratemporal	
Length (right element)	11.9 mm
Width (between the posterolateral process of parietal and the squamosal – right	3.75 mm

element)	
Quadrate	
Maximum height (left element)	20.1 mm
Maximum diameter of the quadrate foramen (left element)	6 mm
Maximum lateromedial width at the articular portion (left element)	10.7 mm
Occiput	
Paroccipital process length (left element)	15.7 mm
Post-temporal fenestra length (left element)	15 mm
Post-temporal fenestra maximum height (left element)	4.1 mm
Lower jaw	
Total length (from the anterior tip of the dentaries to the posterior limits of the articular – right mandibular ramus)	118 mm
Dentary length (as exposed – right element)	45.38 mm
Mandibular fenestra length (left mandible)	24.7 mm
Mandibular fenestra height (left mandible)	8.3 mm

Figure 1. UNIPAMPA 653, holotype of *Teyujagua paradoxa*, skull in right lateral (A), left lateral (B) and dorsal (C) views.

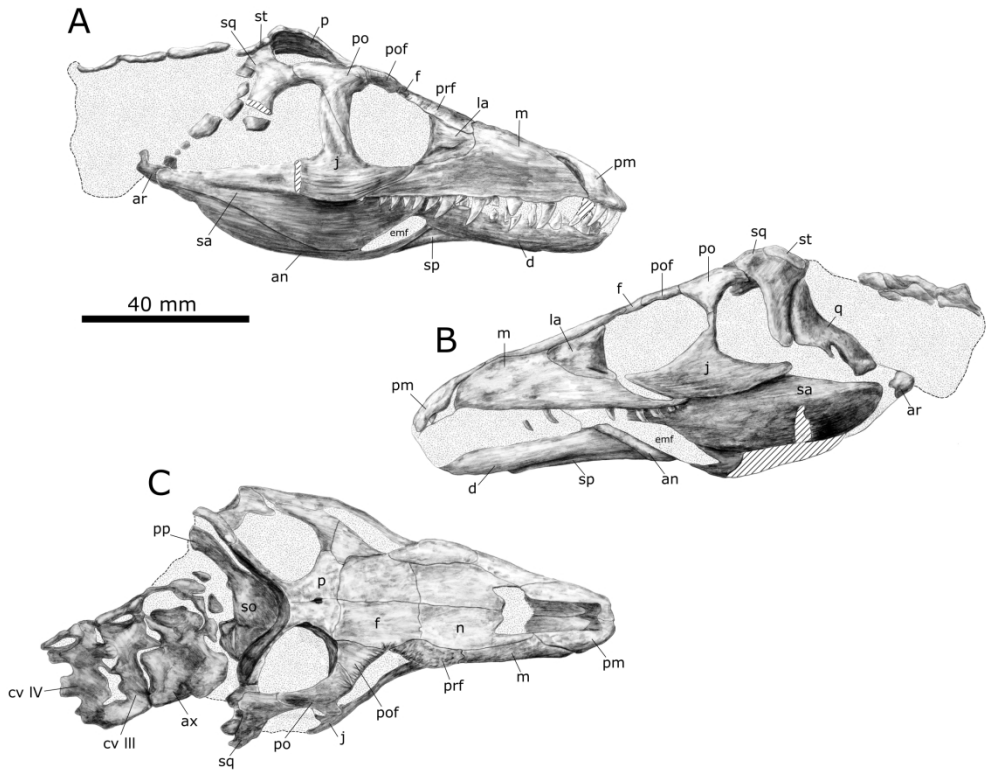

Figure 2. UNIPAMPA 653, holotype of *Teyujagua paradoxa*, interpretative drawings of skull in right lateral (A), left lateral (B) and dorsal (C) views. Abbreviations: an, angular; ar, articular; ax, axis; cv, cervical vertebra; d, dentary; emf, external mandibular fenestra; f, frontal; j, jugal; la, lacrimal; m, maxilla; n, nasal; p, parietal; pm, premaxilla; po, postorbital; pof, postfrontal; pp, paraoccipital process; prf, prefrontal; q, quadrate; sa, surangular; so, supraoccipital; sp, splenial; sq, squamosal; st, supratemporal. Artwork by Joana Bruno.

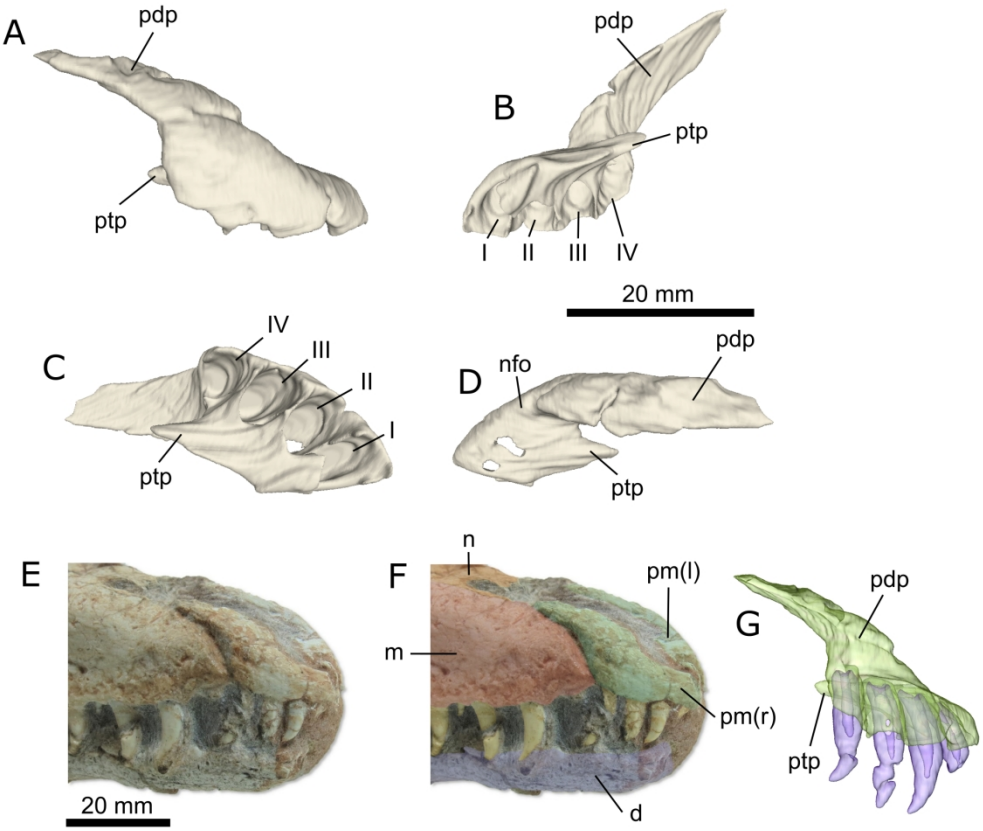

Figure 3. Premaxilla of holotype of Teyujagua paradoxa (UNIPAMPA 653). Right premaxilla in lateral (A), medial (B), ventral (C) and dorsal (D) views; anterior skull bones in dorsolateral view (E, F); rendering of the right premaxilla with teeth inserted (G). Abbreviations: I-IV, premaxillary tooth positions I-IV; d, dentary; m, maxilla; n, nasal; nfo, nasal fossa; pdp, posterodorsal process of premaxilla; pm, premaxilla; ptp, palatal process of premaxilla.

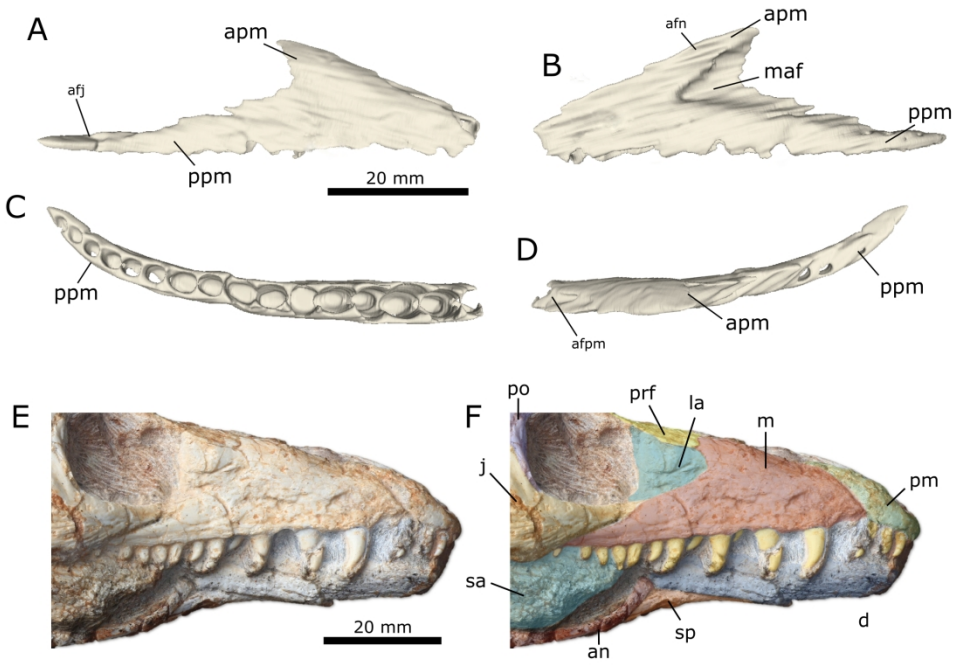

Figure 4. Maxilla of holotype of Teyujagua paradoxa (UNIPAMPA 653). Right maxilla in lateral (A), medial (B), ventral (C) and dorsal (D) views; photograph (E) and interpretative diagram (F) of anterior skull bones in right lateral view. Abbreviations: afj, articulation facet with jugal; afn, articulation facet with nasal; afpm, articulation facet with premaxilla; an, angular; apm, ascending process of maxilla; d, dentary; j, jugal; la, lacrimal; m, maxilla; maf, medial antorbital fossa; pm, premaxilla; po, postorbital; ppm, posterior process of maxilla; prf, prefrontal; sa, surangular; sp, splenial.

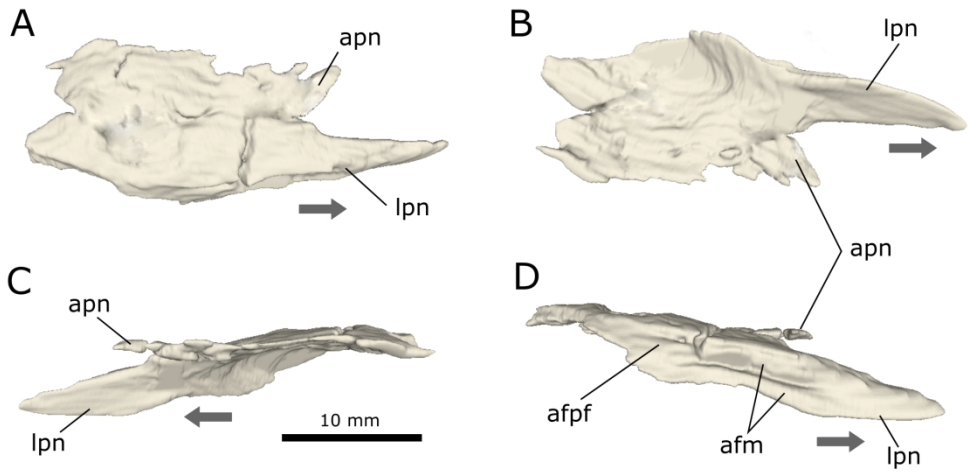

Figure 5. Nasal of holotype of Teyujagua paradoxa (UNIPAMPA 653). Right nasal in dorsal (A), ventral (B), medial (C) and lateral (D) views. Abbreviations: afm, articulation facet with maxilla; afpf, articulation facet with prefrontal; apn, anterior process of nasal; lpn, lateral process of nasal. Arrows indicate anterior direction.

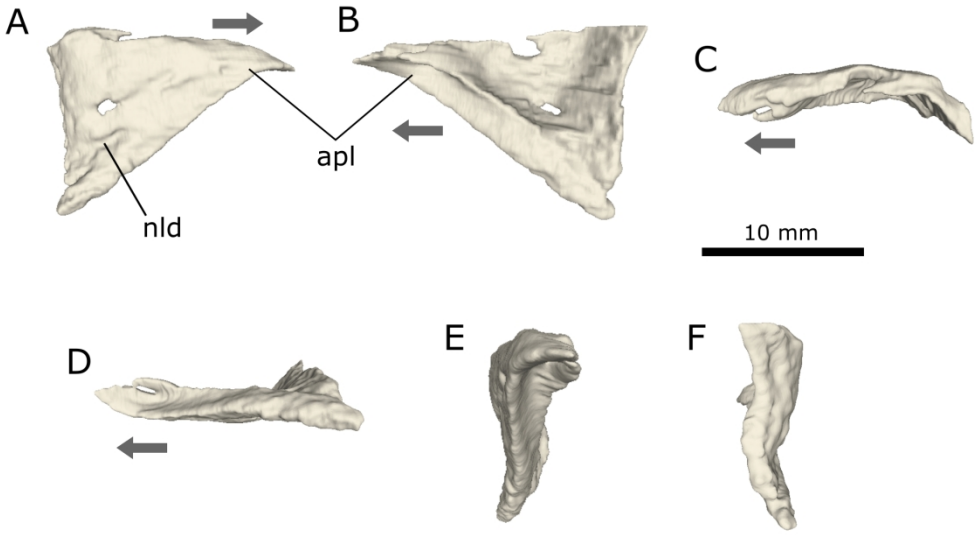

Figure 6. Lacrimal of holotype of Teyujagua paradoxa (UNIPAMPA 653). Right lacrimal in lateral (A), medial (B), dorsal (C), ventral (D), anterior (E) and posterior (F) views. Abbreviations: apl, anterior process of lacrimal; nld, nasolacrimal duct. Arrows indicate anterior direction.

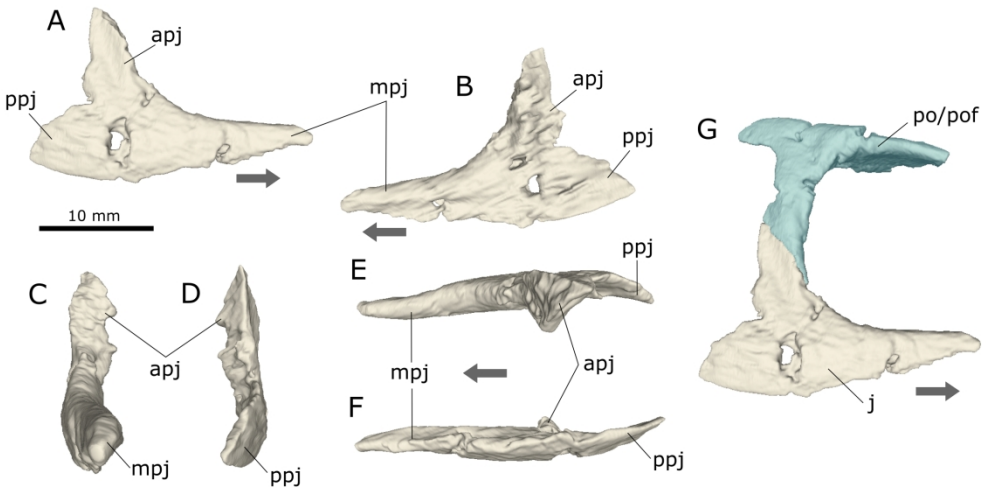

Figure 7. Jugal, postorbital and postfrontal of holotype of Teyujagua paradoxa (UNIPAMPA 653). Right jugal in lateral (A), medial (B), anterior (C), posterior (D), dorsal (E) and ventral (F) views; jugal in articulation with postorbital and postfrontal in lateral (G) view. Abbreviations: apj, ascending process of jugal; j, jugal; mpj, maxillary process of jugal; po, postorbital; pof, postfrontal; ppj, posterior process of jugal. Arrows indicate anterior direction.

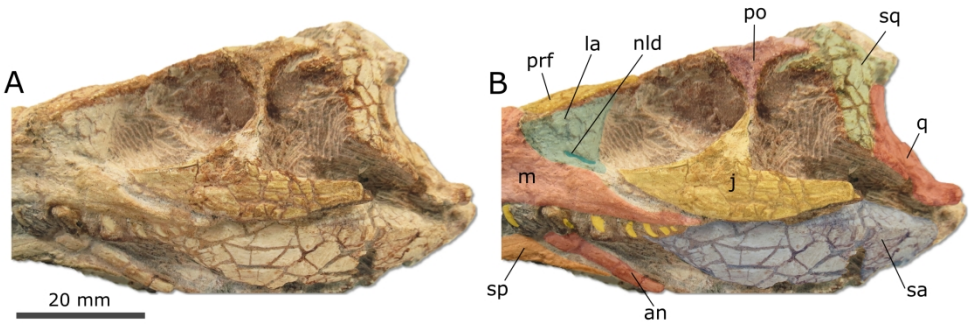

Figure 8. Holotype of Teyujagua paradoxa (UNIPAMPA 653). Photograph (A) and interpretative diagram (B) of posterior skull bones in left lateral view. Abbreviations: an, angular; la, lacrimal; m, maxilla; nld, nasolacrimal duct; po, postorbital; prf, prefrontal; q, quadrate; sa, surangular; sp, splenial; sq, squamosal.

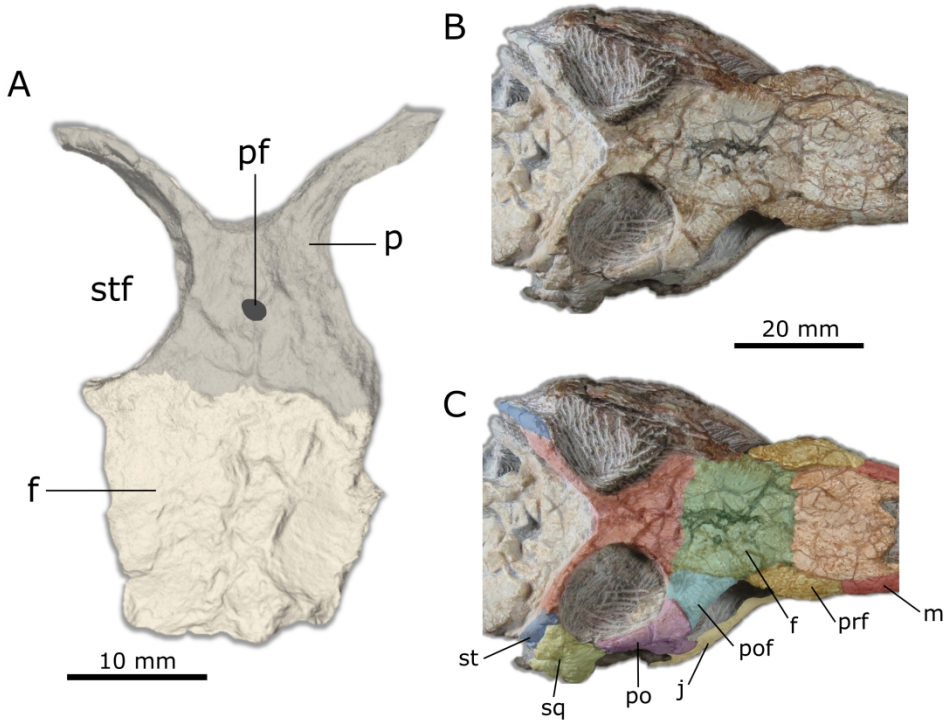

Figure 9. Holotype of Teyujagua paradoxa (UNIPAMPA 653). Frontals and parietals in dorsal view (A); photograph (B) and interpretative diagram (C) of posterior skull bones in dorsal view. Abbreviations: f, frontal; j, jugal; m, maxilla; p, parietal; pf, parietal foramen; pof, postfrontal; po, postorbital; prf, prefrontal; sq, squamosal; st, supratemporal; stf, supratemporal fenestra.

Figure 10. Holotype of Teyujagua paradoxa (UNIPAMPA 653). Dorsal view of the skull detailing circumorbital ornamentation (arrowheads).

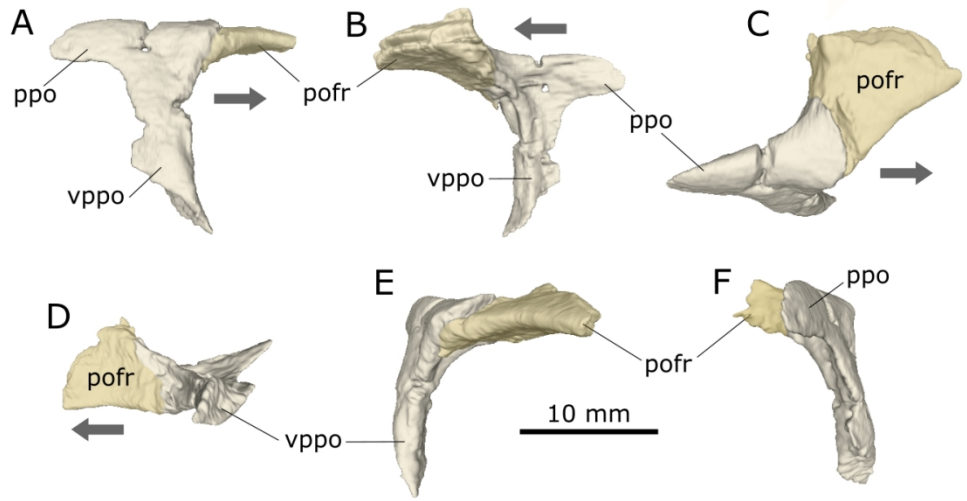

Figure 11. Postorbital and postfrontal of holotype of Teyujagua paradoxa (UNIPAMPA 653). Right postorbital and postfrontal in right lateral (A), medial (B), dorsal (C), ventral (D), anterior (E) and posterior (F) views. Abbreviations: pofr, postfrontal; ppo, posterior process of postorbital; vppo, ventral process of postorbital. Arrows indicate anterior direction.

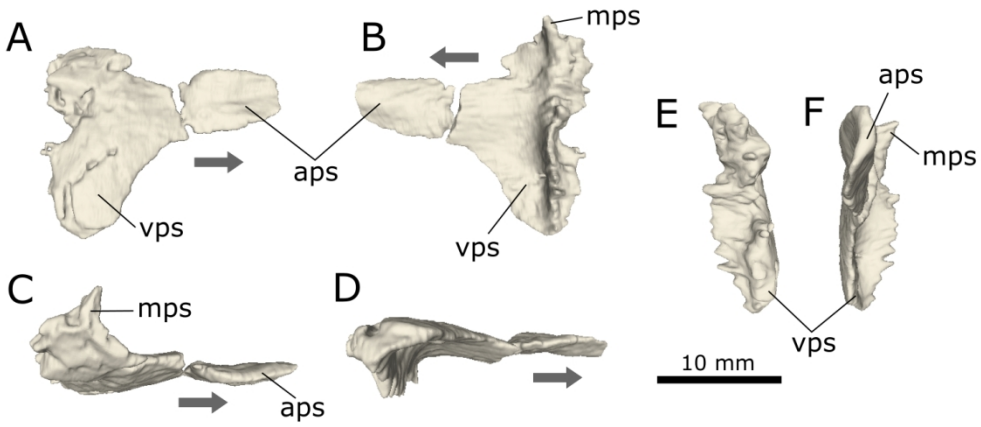

Figure 12. Squamosal of holotype of Teyujagua paradoxa (UNIPAMPA 653). Right squamosal in lateral (A), medial (B), dorsal (C), ventral (D), posterior (E) and anterior (F) views. Abbreviations: aps, anterior process of squamosal; mps, medial process of squamosal; vps, ventral process of squamosal.

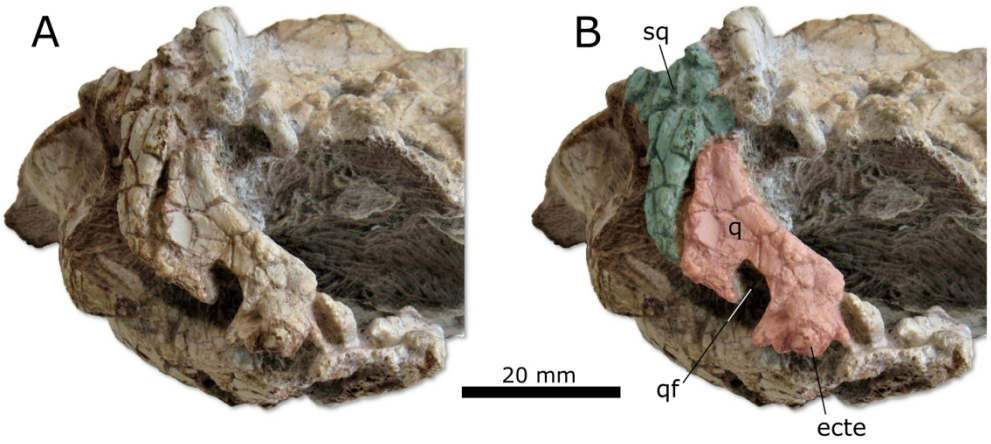

Figure 13. Posterolateral photograph (A) and interpretative diagram (B) of the skull of holotype of Teyujagua paradoxa (UNIPAMPA 653), detailing the left quadrate and squamosal. Abbreviations: ecte, ectepicondyle; q, quadrate; qf, quadrate foramen; sq, squamosal.

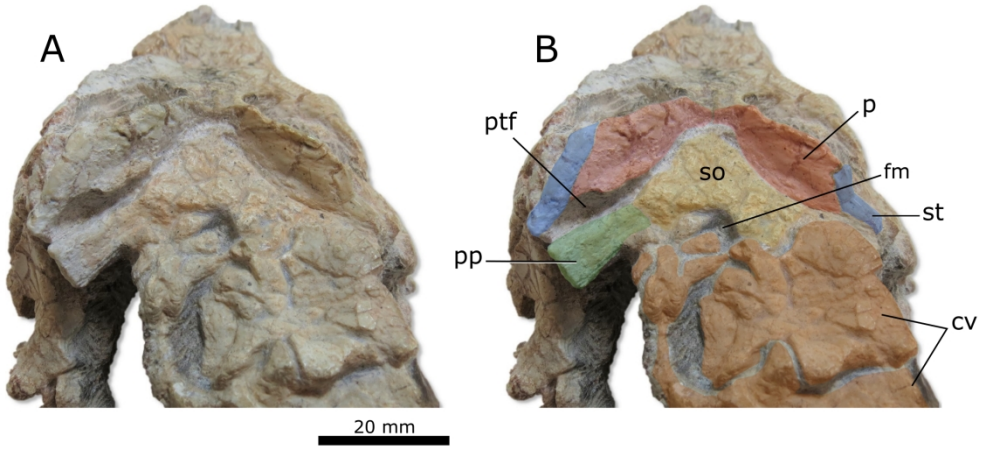

Figure 14. Posterodorsal photograph (A) and interpretative diagram (B) of holotype of Teyujagua paradoxa (UNIPAMPA 653) detailing occipital bones. Abbreviations: cv, cervical vertebrae; fm, foramen magnum; p, parietal; pp, paroccipital process; ptf, post-temporal fenestra; so, supraoccipital; st, supratemporal.

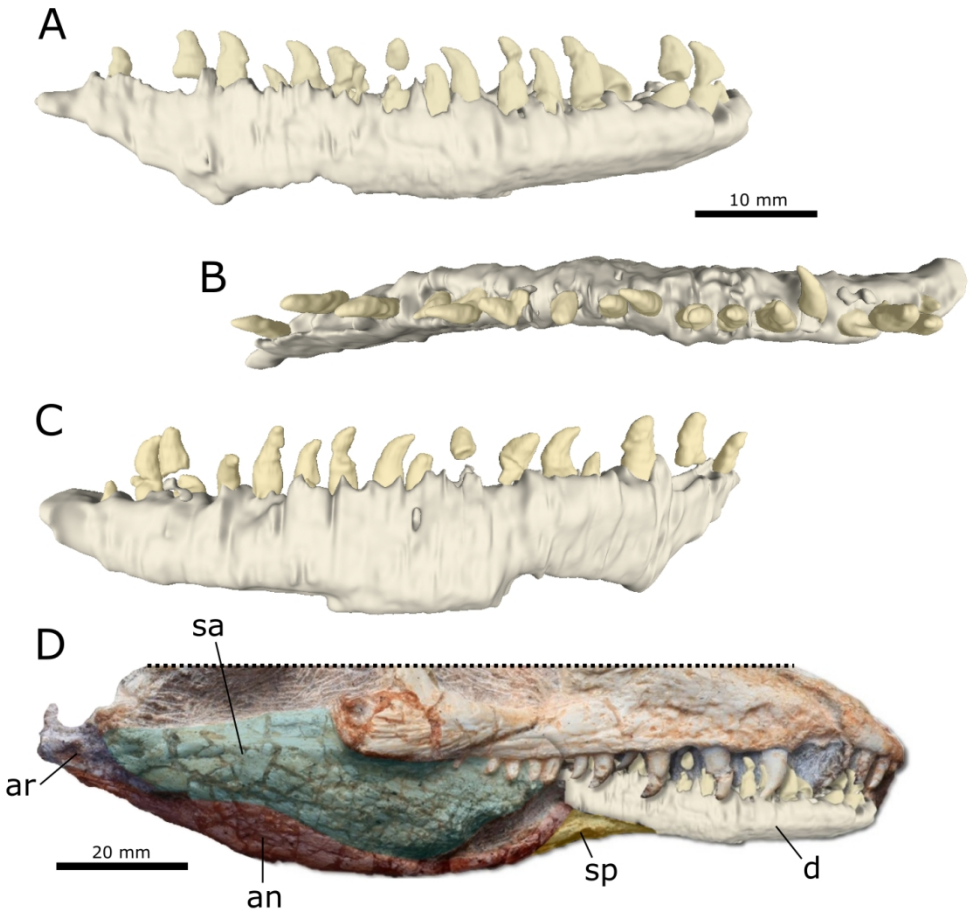

Figure 15. Lower jaw of holotype of Teyujagua paradoxa (UNIPAMPA 653). Right dentary and articulated splenial after rendering in lateral (A), dorsal (B) and medial (C) views; interpretative diagram (D) of lower jaw in right lateral view, with artificial insertion of dentary rendering Abbreviations: an, angular; ar, articular; d, dentary; sa, surangular; sp, splenial.

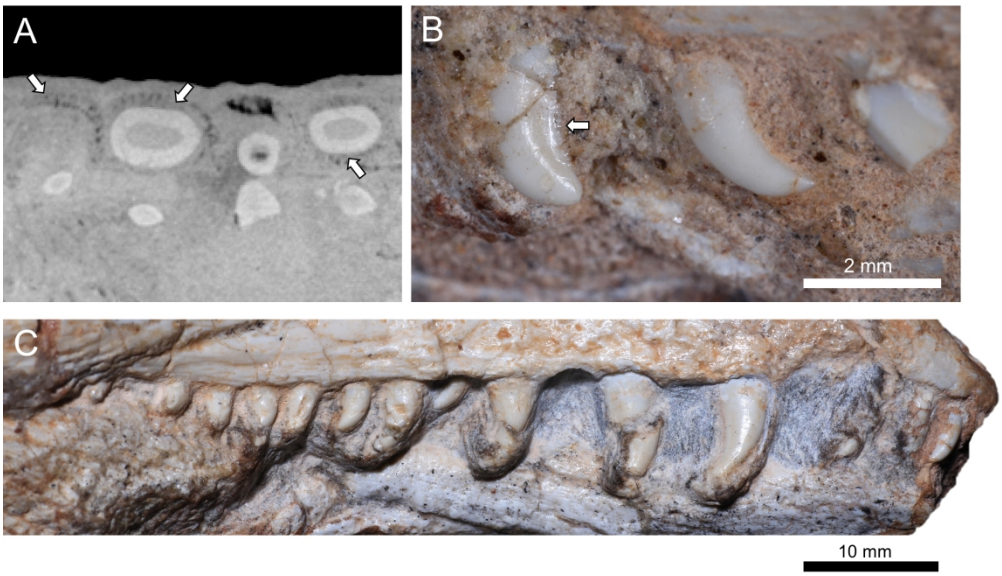

Figure 16. Marginal dentition of holotype of Teyujagua paradoxa (UNIPAMPA 653). Tomographic slice of marginal dentition in transverse section (A), arrows indicate bone striae ankylosing the teeth to surrounding alveoli; photograph of posterior maxillary teeth in lateral view (B), the arrow indicates serrations associated with the distal carina; marginal maxillary and premaxillary dentition in right lateral view (C).

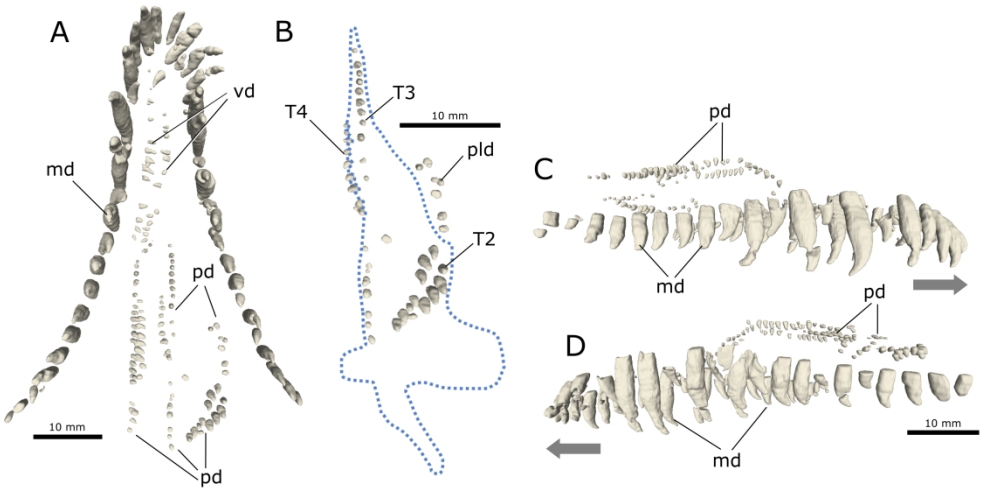

Figure 17. Marginal and palatal dentition of holotype of Teyujagua paradoxa (UNIPAMPA 653). Dentition in palatal view (A); teeth associated with left pterygoid and palatine in palatal view (B); dentition in right lateral (C) and left lateral (D) views. Arrows indicate anterior end of the skull; dashed line indicates inferred pterygoid outline. Abbreviations: T2-T4, pterygoid tooth fields according to Welman (1998); md, maxillary dentition; pd, palatal dentition; pld, palatine dentition; vd, vomerine dentition.

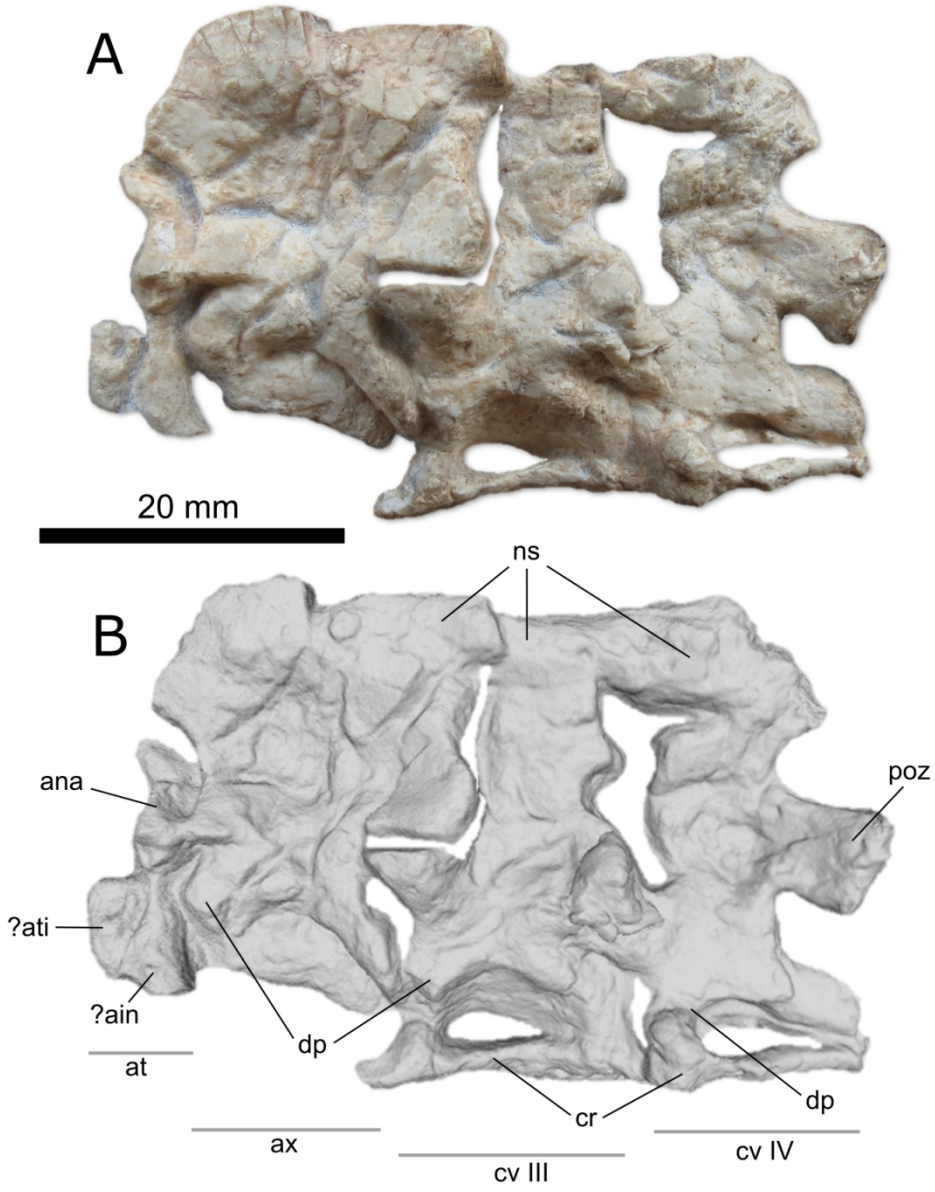

Figure 18. Photograph (A) and digital rendering (B) of cervical vertebrae of holotype of Teyujagua paradoxa (UNIPAMPA 653) in left lateral view. Abbreviations: ain, axis intercentrum; ana, atlas neural arch; at, atlas; ati, atlas intercentrum. ax, axis; cr, cervical rib; cv III, cervical vertebra III; cv IV, cervical vertebra IV; dp, diapophysis; ns, neural spine; poz, postzygapophysis.

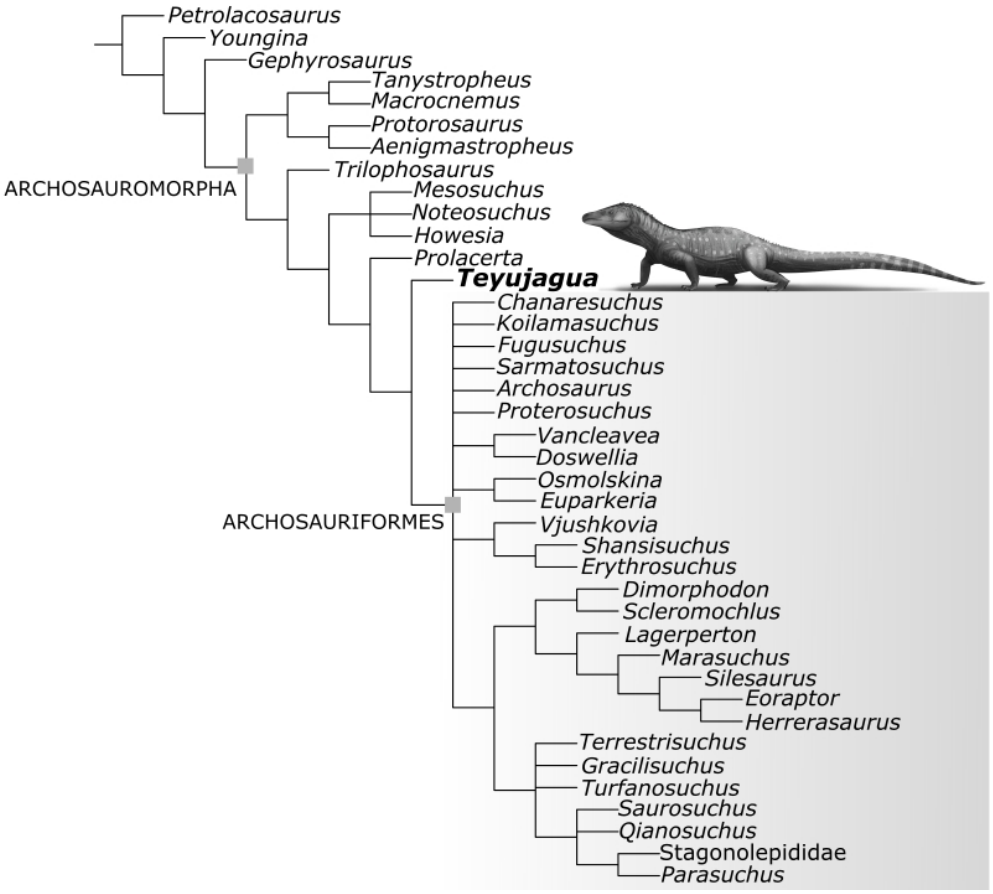

Figure 19. Strict consensus tree recovered by heuristic analysis of the dataset of Pinheiro et al. (2016) including updated scores for Teyujagua paradoxa. Artwork by Márcio L. Castro.

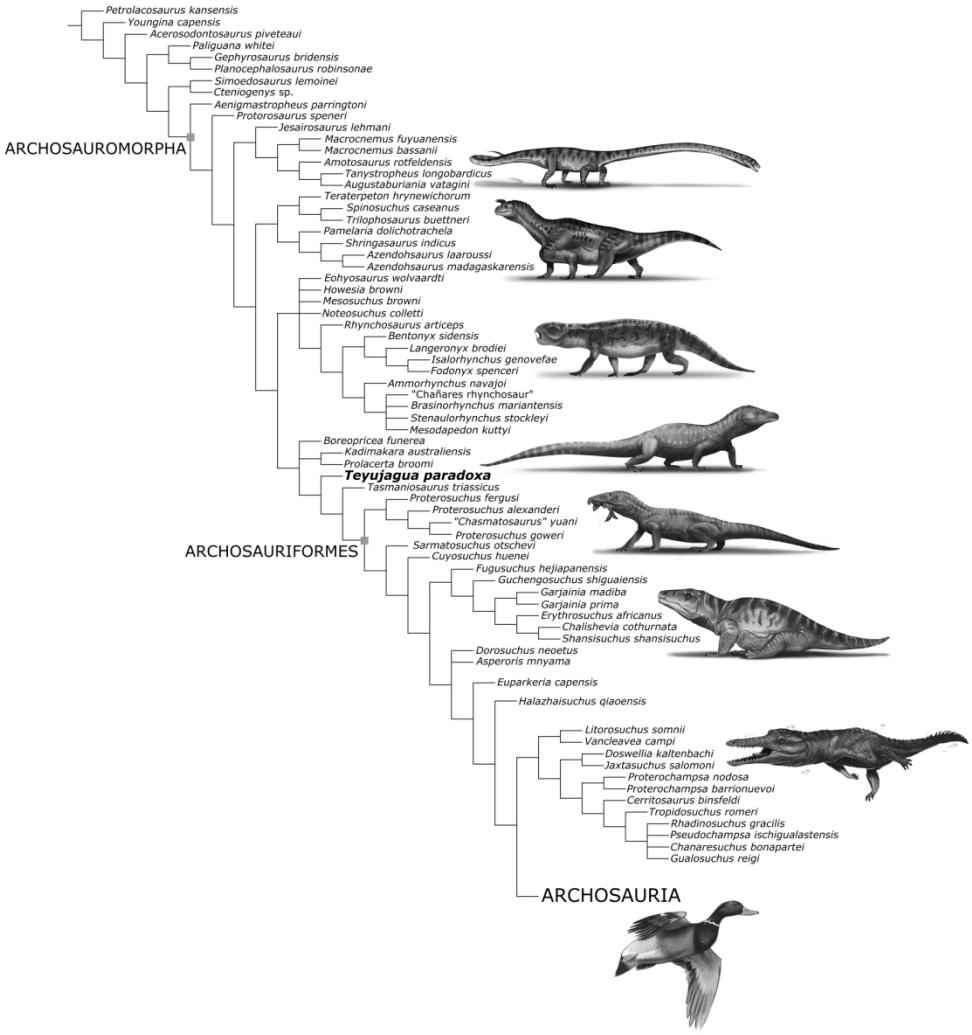

Figure 20. Strict consensus tree recovered by heuristic analysis of the dataset of Butler et al. (2019) including updated scores for Teyujagua paradoxa. Artwork by Márcio L. Castro.

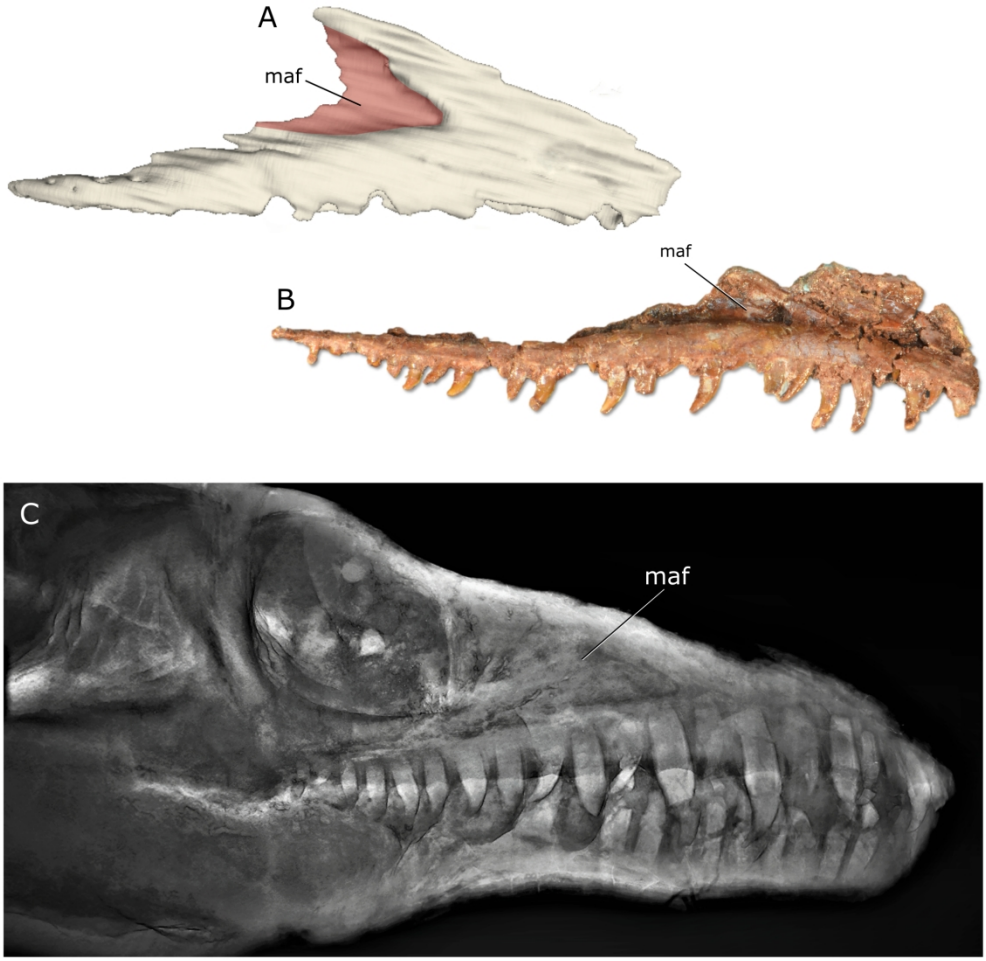

Figure 21. Maxilla of Teyujagua paradoxa (UNIPAMPA 654) (A) (mirrored) and Prolacerta broomi (BP/1/2675) (B) in medial view; μCT-based rendering of rostrum of UNIPAMPA 653 in right lateral view (C), depicting internal structure of the skull. Not to scale. Abbreviation: maf, medial antorbital fossa. Photograph of Prolacerta courtesy of Martín Ezcurra.

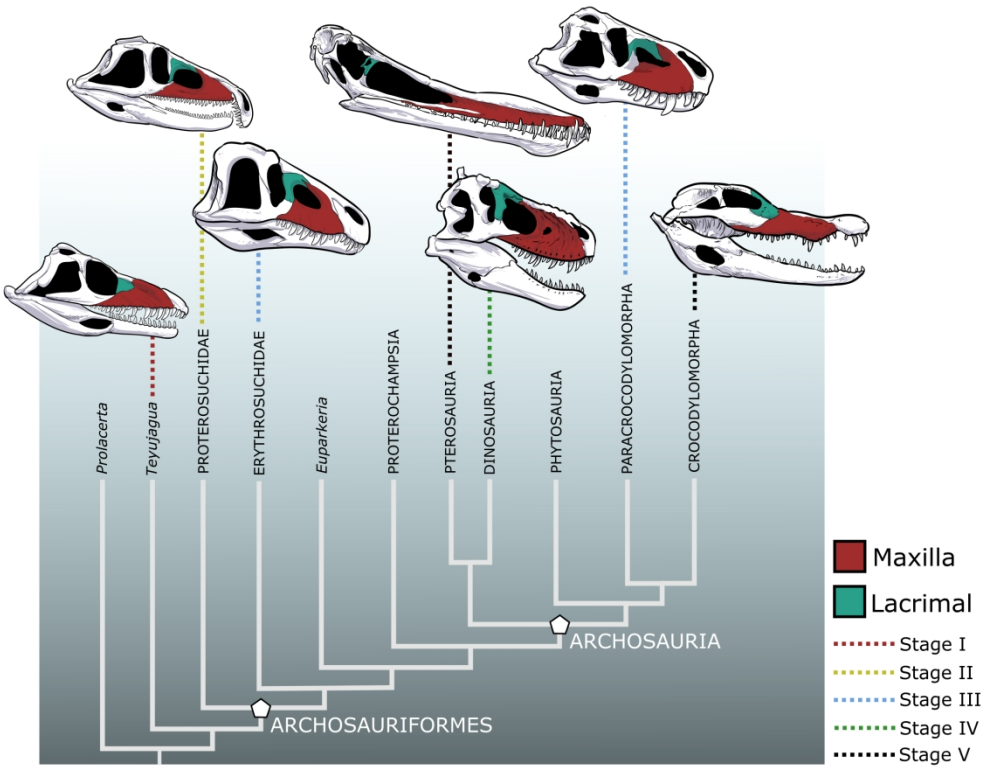

Figure 22. Simplified phylogenetic relationships of selected archosauromorphs, displaying key steps of antorbital fenestrae evolution within the clade. Artwork of skulls by Márcio L. Castro.

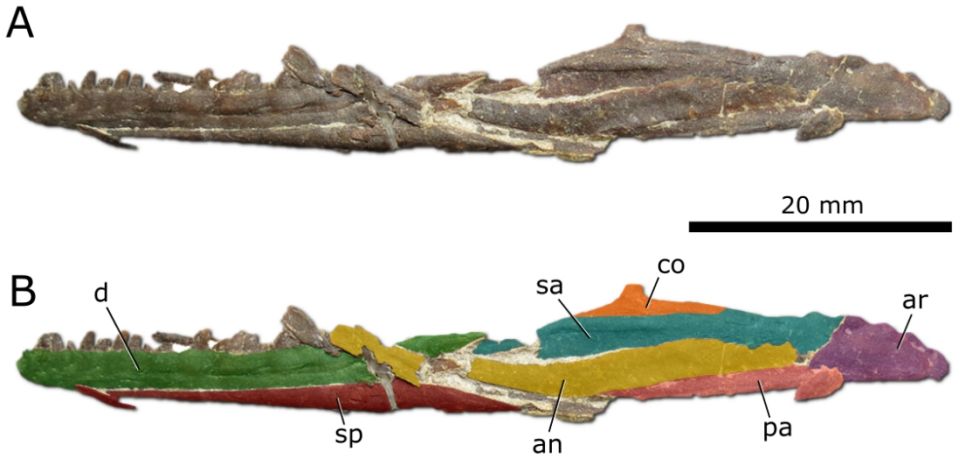

Figure 23. Macrocnemus aff. fuyuanensis (PIMUZ T 1559). Photograph (A) and interpretative diagram (B) of lower jaw in left lateral view. Abbreviations: an, angular; ar, articular; c, coronoid; d, dentary; pa, prearticular; sa, surangular; sp, splenial.

Figure 24. Dawn of the Triassic in southwestern Gondwana. Artistic representation of Sanga do Cabral Formation fauna, with the parareptile Procolophon in the foreground, Teyujagua in the midground and several individuals of the temnospondyl Tomeia in the background. Artwork copyright Mark Witton.